

## **A Cretaceous carbonate delta drift in the Montagna della Maiella, Italy**

GREGOR P. EBERLI<sup>\*</sup>, DANIEL BERNOULLI<sup>†</sup>, ADAM VECSEI<sup>†,‡</sup>, FLAVIO S. ANSEMETTI<sup>†,§</sup>, MARIA MUTTI<sup>†,¶</sup>, GIOVANNA DELLA PORTA<sup>\*\*</sup>, THOMAS LÜDMANN<sup>#</sup>, MARK GRASMUECK<sup>\*</sup> and RIZKY SEKTI<sup>\*,@</sup>

<sup>\*</sup> CSL – Center for Carbonate Research, University of Miami, 4600 Rickenbacker Causeway, Miami, FL 3314 (E-mail: geberli@rsmas.miami.edu)

<sup>†</sup> Department of Earth Sciences, Swiss Federal Institute of Technology (ETH), CH-8092 Zürich, Switzerland

<sup>‡</sup> current address: Tannenweg 23, 8400 Winterthur, Switzerland

<sup>§</sup> current address: Institute of Geological Sciences, University of Bern, Baltzerstrasse 1+3, 3012 Bern, Switzerland

<sup>¶</sup> current address: Institute of Geosciences, University of Potsdam, Karl-Liebnecht-Str. 24-25, 14476 Potsdam-Golm, Germany.

<sup>\*\*</sup> Earth Sciences Department, Milan University, Via Mangiagalli 34, 20131, Milan, Italy.

<sup>#</sup> Institute of Geology, University of Hamburg, Bundesstr. 55, 20146 Hamburg, Germany

<sup>@</sup>current address: ExxonMobil Houston Campus, 22777 Springwoods Village Parkway, Spring, TX 77389, USA

**Associate Editor – Tracy Frank**

**Short Title – Carbonate delta drift, Italy**

### **ABSTRACT**

The Upper Cretaceous (Campanian–Maastrichtian) bioclastic wedge of the Orfento Formation in the Montagna della Maiella, Italy, is compared to newly discovered contourite drifts in the Maldives. Like the drift deposits in the Maldives, the Orfento Formation fills a channel and builds a delta-shaped and mounded sedimentary body in the basin that is similar in size to the approximately 350 km<sup>2</sup> large coarse-grained bioclastic delta drifts in the Maldives. The

This article has been accepted for publication and undergone full peer review but has not been through the copyediting, typesetting, pagination and proofreading process, which may lead to differences between this version and the Version of Record. Please cite this article as doi:

10.1111/sed.12590

This article is protected by copyright. All rights reserved.

composition of the bioclastic wedge of the Orfento Formation is also exclusively bioclastic debris sourced from the shallow-water areas and reworked clasts of the Orfento Formation itself. In the near mud-free succession, age-diagnostic fossils are sparse. The sedimentary textures vary from wackestone to float-rudstone and breccia/conglomerates, but rocks with grainstone and rudstone textures are the most common facies. In the channel, lensoid convex-upward breccias, cross-cutting channelized beds and thick grainstone lobes with abundant scours indicate alternating erosion and deposition from a high-energy current. In the basin, the mounded sedimentary body contains lobes with a divergent progradational geometry. The lobes are built by decametre thick composite megabeds consisting of sigmoidal clinofolds that typically have a channelized topset, a grainy foreset and a fine-grained bottomset with abundant irregular angular clasts. Up to 30 m thick channels filled with intraformational breccias and coarse grainstones pinch out downslope between the megabeds. In the distal portion of the wedge, stacked grainstone beds with foresets and reworked intraclasts document continuous sediment reworking and migration. The bioclastic wedge of the Orfento Formation has been variously interpreted as a succession of sea-level controlled slope deposits, a shoaling shoreface complex, or a carbonate tidal delta. Current-controlled delta drifts in the Maldives, however, offer a new interpretation because of their similarity in architecture and composition. These similarities include: (i) a feeder channel opening into the basin; (ii) an excavation moat at the exit of the channel; (iii) an overall mounded geometry with an apex that is in shallower water depth than the source channel; (iv) progradation of stacked lobes; (v) channels that pinch out in a basinward direction; and (vi) smaller channelized intervals that are arranged in a radial pattern. As a result, the Upper Cretaceous (Campanian–Maastrichtian) bioclastic wedge of the Orfento Formation in the Montagna della Maiella, Italy, is here interpreted as a carbonate delta drift.

**Keywords** Carbonate contourite drift, delta drift, Maiella Mountains, Orfento Formation, prograding lobes.

## INTRODUCTION

During the Late Campanian to the Late Maastrichtian, the coarse-grained bioclastic Orfento Formation was deposited on the margin of the Apulian carbonate platform. Well-sorted bioclastic carbonate sand of mainly rudist debris with little visible cementation is the most abundant lithology of the Orfento Formation but coarse rudist debris, intraformational breccias and conglomerates are also common. The lithostratigraphic unit containing this bioclastic wedge has been defined as the Orfento Formation by Vecsei (1991) and includes the lithostratigraphic unit termed 'Calcari Cristallini' by Catenacci, (1974) and is equivalent to the Orfento Member of the Acquaviva Formation (Crescenti *et al.*, 1969) and 'Barre Jaune' (Accarie, 1988). The bioclastic wedge, which is up to 360 m thick, is a succession of decametre thick prograding lobes with coarse channelized topsets and downlapping foresets (Eberli *et al.*, 1993; Mutti *et al.*, 1996; Vecsei, 1998). The mode of deposition and the depositional environment of the Orfento Formation has been debated for decades because the unique bioclastic nature and

the internal bedding characteristics are hard to reconcile with existing facies models, particularly when the environments below and above the formation are taken into account.

The Orfento Formation buries the escarpment-like Upper Cretaceous platform edge and forms large-scale prograding lobes from the Maiella platform towards the basin (Fig. 1; Eberli *et al.*, 1993, 2004; Mutti *et al.*, 1996; Vecsei *et al.*, 1998; Vecsei, 1998). On the platform, it overlies the bedded, shallow-water deposits of the Cima delle Murelle Formation and nearly fills a depression that formed in the platform during the Early Campanian (Rusciadelli *et al.*, 2003; Morsili *et al.*, 2004). In the basin, the coarse bioclastic succession unconformably overlies the basal deposits of the Tre Grotte Formation, which is a nannofossil-rich periplatform ooze (known as scaglia) with intercalations of thick megabreccias and calcareous turbidites deposited along the escarpment in a deep-water setting (Figs. 1 and 2; Accarie *et al.*, 1986; Vecsei 1991; Eberli *et al.*, 1993; Casabianca *et al.*, 2002; Rusciadelli *et al.*, 2003; Maura 2013). The top of the bioclastic Orfento Formation is an erosional unconformity that is up to 50 m in relief but is seen in many places as shallow channels filled by lithic breccias of possibly Early Palaeocene and Thanetian age intercalated with pelagic limestones (Anselmetti *et al.*, 1997; Vecsei *et al.*, 1998). In the distal portion the Orfento Formation is overlain by a deep-water carbonate turbidite succession (Santo Spirito Formation) with a concave upward geometry that is interpreted as a submarine fan (Vecsei, 1991; Vecsei *et al.*, 1998). Thus, the Orfento Formation is bracketed in the basin between two deep-water successions with turbidites.

Because the bioclastic wedge of the Orfento Formation lacks the classic Bouma-type turbidite sequences, the depositional environment of the Orfento Formation has been interpreted in several different ways. Crescenti *et al.* (1969) state that the coarse carbonate sand has been transported over considerable distances across the platform and the basin. Accarie (1988) who called the Orfento Formation 'Barre Jaune' separated two facies, one with plain to undulate bedding and one with inclined bedding. Accarie (1988) interpreted the first facies as residual deposits from a current that loses its strength to carry its sediment load and the second facies as deposited by a current with intermittent quiet phases. Vecsei (1998) saw the prograding bioclastic lobes on the upper slope as the result of deposition in an ebb-dominated tidal delta, and based this interpretation on the complex internal geometries of the lobes that combine characteristics of unidirectional sandwaves and the alternating point sources of deltas. Vecsei (1998) proposed strong tidal currents or storms as the transporting mechanisms. Eberli *et al.* (1993) envisioned the Orfento Formation as slope apron with four sequences in which the coarse rudstone and channel-filling breccias are the lowstand deposits. Mutti *et al.* (1996) interpreted the Orfento Formation as a prograding margin succession in which sea-level controls architecture, facies and sequence distribution and placed the various facies into a shoreface succession that with each sequence would step down and further basinward. None of these depositional models, however, has so far been able to explain all the observed facies and depositional geometries. The current theory of Accarie and others does not explain the mounded geometry. No modern carbonate tidal delta has the size and shape proposed by Vecsei (1998). A sea-level controlled slope apron as suggested by Eberli *et al.* (1993) is expected to have more periplatform beds between the thick grainstone beds and would hardly show the distinct progradational pattern that is observed in the Orfento Formation. The shoreface model of Mutti *et al.* (1996) explained the downcutting and scouring of grainstone beds but the lack of any evidence of beach facies as the shoreface downsteps into the basin is not explained in this

model. Also, the deep-water breccias and turbidite succession overlying the Orfento Formation makes it difficult to place the formation into a shallow shoreface environment. All models agree that the nearly mud-free and coarse-grained grainstone packages, the abraded rudist components, and the common channeling and 'cannibalization' of the strata document high-energy conditions that need to exist for an extended period of time.

The discovery of a hitherto unknown drift type during Integrated Ocean Drilling Program (IODP) Expedition 359 to the Maldives offers the opportunity to re-examine the succession in the Maiella and to propose a new interpretation of these deposits. Two drift bodies in the Kardiva Channel had been identified before the expedition based on the geometries seen on the seismic data (Lüdmann *et al.*, 2013). The cores retrieved during IODP Expedition 359 revealed a previously undescribed type of coarse-grained drift deposit. These delta drifts form at the mouth of the southern and northern West Kardiva Channel where they open into the Inner Sea and the currents drop their sediment load as current strength dissipates (Lüdmann *et al.*, 2018). The geometry, dimensions and the sedimentary structures of the Kardiva delta drifts are very similar to the Upper Cretaceous coarse-grained carbonate deposits of the Orfento Formation in the Maiella.

The aim of this paper is to present and compare the elements of, and variations between, the prograding delta drifts in the Maldives and the prograding lobes in the Montagna della Maiella. Based on these similarities to the delta drifts in the Maldives the depositional environment of the Orfento Formation a case is made that the bioclastic wedge of the Orfento Formation is a Cretaceous delta drift. The outcrops in the Maiella provide an outcrop-based view that complements the seismic and core data from the Maldives. In the following, the key characteristics of the Orfento Formation are summarized, the existing models are discussed and then the stratal elements and sedimentary structures of Kardiva delta drift in the Maldives are compared with those of the Orfento Formation.

## **DATA SETS AND METHODS**

This study draws on extensive fieldwork conducted in the early 1990s in a project that focused on the sequence stratigraphic analysis of the Cretaceous-Cenozoic platform and basin succession across the Maiella escarpment. Subsequent fieldwork concentrated on the proximal portions of the Orfento Formation (Mutti *et al.*, 1996). In 2006 to 2008, the breccias and turbidites of the Tre Grotte Formation were re-measured and later compared with the bioclastic grainstones and rudstones of the Orfento Formation (Maura, 2013). In 2016, key outcrops were re-visited. Published and unpublished measured sections, maps, outcrops drawings and thin sections analyses from these studies provide a comprehensive data set of the formation. Reconstructing the depositional geometry of the Orfento Formation is based on measured sections published in the following papers (Vecsei, 1991; Eberli *et al.*, 1993; Mutti *et al.*, 1996). In these publications, a surface close to the top of the Orfento Formation was used as the datum. This datum produced an unrealistic steep slope in the basin but preserved a dipping slope for the beds of the Orfento Formation. Here, a sea floor with a slope angle of 5° is placed underneath the sections. This new datum produces a mounded geometry in the bioclastic wedge. The 5° slope might even be steep for a slope consisting of periplatform ooze with intercalations of turbidites and mass gravity flow deposits (Betzler *et al.*, 1999). The slightly higher angle taken is

intended to account for differential compaction of the underlying carbonate ooze of the Tre Grotte Formation (Rusciadelli & Di Simone, 2007).

In the more distal portion, at the Madonna della Mazza quarry, a three-dimensional ground penetration radar (GPR) survey was conducted to visualize the stratigraphy and fractures in the Orfento Formation. Lithology and bedding planes are not easily recognized in outcrop but 3D GPR data reveal both the bedding and sedimentary structures, as well as the different generations of deformation bands with great clarity (Seki, 2010; Marchesini & Grasmueck, 2015). The quarry is 64 m long (east–west), and 50 m wide (north–south) with walls rising about 12 m. Two 3D migrated GPR volumes each 26 x 32 m with a small overlap cover the main level of the quarry. The 3D GPR volumes were simultaneously acquired with a 100 MHz and a 200 MHz GPR System with a line spacing of 25.0 cm and 12.5 cm, respectively. The 100 MHz antenna achieved 21.6 m while the 200 MHz antenna yielded 12 m of penetration (Rizky, 2010; Marchesini & Grasmück, 2015). The survey was conducted using a Mala™ single-channel GPR system (Guideline Geo, Malå, Sweden) coupled to a 3D laser positioning system to achieve centimetre positioning precision. An LED based guidance tool mounted on the antenna guides the antenna operator along the survey tracks (Seki, 2010). The stratigraphic analysis in the quarry is based on the measured sections combined with the GPR for 3D spatial facies analysis. The measured section captures the lithology of the strata and the facies classification based on the texture and composition of the strata in the quarry. The lithofacies is then correlated to the subsurface GPR facies. Thin-section analysis of the outcrop samples provides information on texture, diagenesis and grain types of the strata.

A comparative sedimentology approach is performed between the bioclastic wedge of the Orfento Formation and delta drifts from the Maldives based on seismic and core data from IODP Expedition 359 to the Maldives (Betzler *et al.*, 2016a; Lüdmann *et al.*, 2018). The seismic data along was collected during the *R/V Meteor* cruise M74/4 in December 2007: 1400 km of high-resolution reflection seismic data were obtained using a Hydrosience Technologies Inc. (Mineral Wells, Texas, USA) 144 channel digital streamer array (Lüdmann *et al.*, 2013). The acquisition of the core material and associated data sets are described in Betzler *et al.* (2016a).

## REGIONAL SETTING

### The southern Apennine platforms and seaways in the Late Cretaceous

In the Late Triassic and Early Jurassic, the southern Adria domain experienced crustal extension that resulted in the break-up of a large carbonate shelf on the Apulian microplate and the formation of a series of isolated carbonate platforms and intervening basins (e.g. Bernoulli, 1972; Bernoulli, 2001). In the Maiella area, the Lagonegro–Molise Basin separated the Apulian platforms from the internal Apenninic platforms (Abruzzi-Lazio-Campania platforms) (Fig. 2A; Iannace & Zamparelli, 2002; Vitale *et al.*, 2017). The Adriatic microplate experienced a second episode of extension in the Late Cretaceous–Palaeogene that Vitale *et al.* (2017) call an abortive rifting stage. The renewed extension created topography on some platforms, widened the seaways between the platforms and increased circulation of the ocean currents through the Tethyan realm (Poulson *et al.* 1996; Föllmi & Delamatte, 1991). In this time period falls the

segmentation of the Apulian platform margin in the Maiella, resulting in partial drowning of the Maiella margin and the formation of an 'intra-platform seaway' across the northern margin (Sanders, 1994; Rusciadelli *et al.*, 2003; Rusciadelli & Ricci, 2008). This event in the Late Cretaceous probably enlarged or deepened the Adriatic basin (Mostardini & Merlini, 1986; Zappaterra, 1994).

### **The Maiella platform margin**

The north-western margin of the Apulian platform is exposed in the Montagna della Maiella, Italy (Fig. 2B). The transition between the Cretaceous platform and the adjacent Marche/Umbria Basin is a spectacularly exposed, roughly west–east trending escarpment (Bally, 1954; Crescenti *et al.*, 1969; Accarie *et al.*, 1986; Accarie, 1988; Vecsei, 1991; Eberli *et al.*, 1993; Vecsei *et al.*, 1998; Rusciadelli *et al.*, 2003). This escarpment probably extends to the Montagna di Morrone in the west but is not exposed. Between both mountains runs the Caramanico Fault cutting across the exposed anticline that pushes the margin by 3500 m into the subsurface (Ghisetti & Vezzani, 2002; Patacca & Scandone, 2007; Patacca *et al.*, 2008). The approximately north–south trending fault, however, exposes a cross-section across the platform and the margin, revealing the facies from the basin, across the margin and into the platform interior (Eberli *et al.*, 1993; Sanders, 1994; Stössel, 1999; Morsili *et al.*, 2002). The Lower Cretaceous platform is composed of shallow-water, mud-rich limestone cycles (Morrone di Pacentro Formation) that extend to the marginal escarpment where they are overlapped by deep-water deposits of the Tre Grotte Formation (Figs 1 and 2). The platform growth is interrupted from the late Albian to middle/late Cenomanian by emersion, karstification and the formation of bauxite (Crescenti *et al.*, 1969; Accarie & Delamatte, 1991). A 5° tilt is associated with this 'mid-Cretaceous' unconformity (Fig. 1), indicating the onset of the extensional tectonic activity in the Late Cretaceous in this part of the Adriatic plate (Vitale *et al.*, 2017). This extension is seen as a series of normal faults that produce a kilometre-scale 'horst and graben' topography on the Maiella platform with a pronounced high along the Monte Acquaviva/Focalone axis (Accarie, 1988). During the subsequent flooding the Middle to Late Cenomanian Cima delle Murelle Formation was deposited with rudist biostromes and bioclastic grainstones along the outer platform and finer-grained and partly mud-rich facies in the inner platform (Sanders, 1994; Stössel, 1999). The variable thickness of coeval platform margins and interior cycles documents depositional topography and unfilled accommodation space during times of small amplitude sea-level changes (Eberli, 2013).

Another platform emergence during the Early to middle Campanian terminated shallow-water platform aggradation (Accarie, 1988; Eberli *et al.*, 1993; Mutti, *et al.* 1996; Stössel, 1999). At this time, an approximately 100 m high escarpment still separated the exposed platform from the basinal deposits of the Tre Grotte Formation (Fig. 1). The exposure is tied to a second major tectonic phase around the Santonian–Campanian boundary that dissected the Apulian platform and enlarged the basins between the platforms on the Adriatic plate (Vitale & Ciarcia, 2013). In the Gargano area, a topography of emergent areas and drowned portions of the platform was created (Morsili *et al.*, 2002, 2004). Likewise, the Maiella platform margin was segmented, creating highs and lows, in particular a depression next to the Monte Rotondo that is called an 'intraplatform sea-way' by Mutti (1995) and 'drowning seaway' by Rusciadelli *et al.* (2003), and is hereafter called the 'Rotondo Channel' (Fig. 3). In the Upper Campanian, the platform was

flooded again and rudists became the main component of the Upper Campanian–Maastrichtian Orfento Formation. The formation consists of poorly cemented, highly porous grainstones, mainly composed of rudist debris, ranging in size mostly from silt to coarse sand, but pebble to boulder size clasts are found in channelized breccias (Vecsei 1991; Mutti *et al.* 1996). The large prograding carbonate wedge of the Orfento Formation, which is the focus of this study, buries the escarpment of Upper Cretaceous platform and nearly fills the Rotondo Channel which also acts as a feeder channel for the bioclastic wedge (Accarie *et al.*, 1986; Sanders, 1994; Mutti, 1995; Mutti *et al.*, 1996; Vecsei, 1998; Rusciadelli *et al.*, 2003; Morsili *et al.*, 2004). An erosional unconformity marks the top of the Orfento Formation. The unconformity is overlain by an up to 170 m thick, deep water succession of breccias with lithoclasts, biotrital grainstones and pelagic limestones of the Santo Spirito Formation (Fig. 1; Vecsei, 1991). No persistent shallow-water platform was established between the latest Maastrichtian and middle to late Ypresian. However, slide blocks of upper Danian–lower Thanetian corallgal reefs are preserved at the base of the Santo Spirito Formation along the northern flank of Valle delle Tre Grotte (Moussavian & Vecsei, 1995). North of the former platform Early Eocene deposition continued to be mostly lithoclastic breccias and calcareous turbidite in pelagic limestones while a foraminifera grainstone shoal was deposited on the platform (Alveolina Limestone of Bally, 1954). In earliest Priabonian time, slope carbonates were deposited in the entire northern Montagna della Maiella which during the early Priabonian prograded northward with small patch reefs. In the early Oligocene, reefs prograded at least 4 km basinward over the gently inclined upper slope and in the latest Oligocene–Early Miocene a gently inclined shelf was established (Bolognano Formation; Brandano *et al.*, 2016). The Messinian desiccation of the Mediterranean ended carbonate deposition. During the orogeny of the Apennines in the Early Pliocene the platform to basin system became part of a thrust sheet (Ghisetti & Vezzani, 1983, Rusciadelli, 2005). Because the thrust was perpendicular to the Maiella margin, the geometry of the margin and adjacent basin are preserved in a tilted anticline. The deformation does, however, make the exact determination of the palaeoslopes and amount of compaction difficult (Rusciadelli & Simone, 2007).

## RESULTS

The Upper Campanian–Maastrichtian Orfento Formation is different in its composition and geometry from the underlying and overlying platform and basin successions (Fig. 4). It is composed of bioclastic grainstones to rudstones, sourced almost exclusively from rudist fragments and breccias with clasts from the Orfento Formation. The underlying Tre Grotte Formation contains few rudist debris but consists of fine-grained periplatform ooze ('scaglia' of Italian authors), carbonate turbidites and megabreccias mostly composed of platform lithoclasts (Fig. 4A and B) (Cresenti *et al.*, 1969; Accarie, 1988; Casabianca *et al.*, 2002, Rusciadelli *et al.*, 2003, Maura, 2013). The calcareous turbidites in the Tre Grotte Formation are generally thin-bedded T<sub>b</sub> and T<sub>c</sub> type turbidites (Fig. 4C). The scaglia contains abundant nannofossils and foraminifera, documenting a deep-water environment but a scarcity of bioclastic debris from the platform (Fig. 4D). Yet, the coeval platform margin contains abundant rudist buildups that are partly reworked by tidal currents, forming cross-bedded grainstone and rudstone cycles, and bioclastic sand waves (Sanders 1994; Stössel, 1999, Eberli, 2010). This scarcity indicates that offbank transport of rudist debris was minimal. In contrast, the Orfento Formation is

mostly composed of rudist debris while breccias with platform lithoclasts are restricted to the base of the Rotondo Channel and to a few up to 50 cm thick beds at the base of the formation (Vecsei, 1991, 1998). The abrupt change of composition and bedding character to the coarse-grained nature of the bioclastic Orfento Formation indicates a fundamental change in depositional processes from mass gravity flows into fine-grained periplatform ooze to the thick-bedded, prograding bioclastic wedge of the Orfento Formation.

### **Dimensions of the bioclastic wedge of the Orfento Formation**

Approximately 150 km<sup>2</sup> of the prograding bioclastic wedge of the Orfento Formation is exposed in the thrust sheet of the Montagna della Maiella (Fig. 5). Outcrops expose the wedge for 15 km from the platform northward into the basin, but the outer edge of the wedge is not exposed. In an east–west direction 10 km are exposed but again, the outcrops do not cover the fringes (Fig. 5). In a core description (Well Vallecupa 45) about 20 km to the north of the escarpment, pelagic limestones (scaglia) with occasional redeposited calcareous grainstones with shallow water biota are reported. These grainstones are likely to be the distal tongues of the bioclastic wedge of the Orfento Formation.

Section heights of the Orfento Formation at several locations display the thickness variations, revealing a mounded sedimentary body (Fig. 6). In each of these sections the Orfento Formation is bracketed by the Tre Grotte Formation at the base and the overlying Santo Spirito Formation. Thus, the thickness variation is not a result of post-orogenic erosion. In the basin, the thickness of the exposed Orfento Formation is thinnest in the proximal position close to the platform margin. The wedge thickens towards the basin, reaching a maximum thickness of 360 m, 6 to 7 km from the mouth of the Rotondo Channel at the Santo Spirito and Maielletta locations (Crescenti *et al.*, 1969; Vecsei, 1991). From this apex, the sections thin both further to the north and to the east and west (Fig. 5). The reduced sedimentary thickness just off the platform is due to an excavation moat at this position (Fig. 6) (Eberli *et al.*, 1993). On the western side of the Montagna della Maiella the thickness is 120 m (Vecsei, 1991), while in the easternmost outcrop (Valle di Pennapiedimonte) the formation is 160 m thick (Lampert *et al.*, 1997; Antonellini *et al.*, 2008). Overall, this thickness distribution indicates a mounded, delta-shaped body that probably was 300 to 450 km<sup>2</sup> in size and 360 m thick in its apex (Figs 5 and 6).

The bioclastic wedge is also nearly filling the Rotondo Channel that was approximately 200 m deep and 1500 m wide, and is today situated between the Monte Rotondo in the west and the Cima delle Murelle/Monte Acquaviva in the east (Fig. 3). The channel cuts through the Maiella platform margin into the Marche-Umbria Basin in the north but also widens to the south (Sanders, 1994).



## Sequence architecture of the Orfento Formation

The Orfento Formation is also a supersequence (Orfento Supersequence) with erosional unconformities at the base and the top (Vecsei, 1991; Eberli *et al.*, 1993; Bernoulli *et al.*, 1996, Vecsei *et al.*, 1998). The basal unconformity is an onlap onto the remaining platform escarpment and an erosional downcut in the proximal basin. Further basinward the lower megasequence boundary is mostly a conformable but associated with a facies change from periplatform ooze to the coarse-grained deposits of the Orfento Formation (Fig. 4). The boundary is associated with a significant hiatus, spanning most of the Campanian *G. ventricosa* zone (Lampert *et al.*, 1997). The unconformity on top of the Orfento Formation is a regional unconformity from the platform across the bioclastic wedge into the basin. The erosion truncates the prograding and inclined beds and removes up to 50 m of the Orfento Formation, which at Monte Belvedere leaves an erosional remnant that is overlapped by the overlying Santa Spirito Formation (Fig. 7). No exposure horizon is recognized on top of Orfento Formation, yet secondary porosity and silicification are present (Mutti 1995). In the valley near Pennapiedimonte, the unconformity is not obvious but the absence of Chron C29r documents non-deposition or erosion during the latest Maastrichtian (Lampert *et al.*, 1997). Within the Orfento Supersequence four sequences are identified. In the proximal (>5 km) position the sequence boundaries are marked by downcutting channels that are filled with amalgamated breccias and rudstones (Vecsei 1991; Eberli *et al.*, 1993; Mutti *et al.*, 1996).

## Biostratigraphic content of the Orfento Formation

One characteristic of this up to 360 m thick bioclastic wedge is the sparsity of age-diagnostic fossils. Some inoceramids are found but ammonites are not present (Accarie, 1988) and calcareous nannofossils that are common in the underlying pelagic deposits of the Tre Grotte Formation are no longer present. The sections close to the platform margin generally lack age-diagnostic fossils all together so that the age of the formation is bracketed from the age determined in the top and bottom of the underlying and overlying strata, respectively (Vecsei, 1991). With increasing distance from the margin, benthic and planktonic foraminifera, in particular globotruncanids, are present in the sections, allowing biozones to be identified (Vecsei, 1991). To the east, where the Orfento Formation thins to about 160 m (Pennepiedamonte), nannofossils are common which, together with magnetostratigraphy, provide a robust age model for the formation (Lampert *et al.*, 1997). Here, the age and duration of the Orfento Formation is from the Late Campanian (Globotruncanita calcarata zone) to Late Maastrichtian (within Abatomphalus mayaroensis zone, Chron C30) (Vecsei, 1991, 1998; Lampert *et al.*, 1997).

## Facies of the Orfento Formation

Ten facies are present in the bioclastic wedge of the Orfento Formation, but the most abundant facies is what Catenacci (1974) called 'calacare cristallini' and what Crescenti *et al.* (1996) describe as: "typical crystalline white calcarenites with a homogeneous middle grain size arranged in beds of some meter thickness ... highly porous in the north (basin). ... The grains

originate from broken and reworked biotrital material of shallow rudist reefs that are transported across a large neritic area to the pelagic realm” (loosely translated from Crescenti *et al.*, 1969). In addition to fragments from rudists (*Hippuritidae* and *Radiolitidae*), skeletal debris from echinoids, inoceramids and benthic foraminifera (*Orbitoides media*, *Siderolites calcitrapoides*, *Omphalocyclus macroporus* and *Hellenocyclina beotica*) are found and, in the more distal section, sponge spicules, calcispheres and small benthic foraminifera are part of the biotritus.

The 10 facies (Fa1 to Fa10) are listed in Table 1, nine of these facies are illustrated in Fig. 8 and their distribution along the prograding edge is given in Fig. 9. The facies fall into two major groups. The grainstone group is the primary facies and is typically fine to coarse sand size but consists of variable sedimentary structures. Massive grainstone beds can be up to 5 m in thickness. They are often capped by a mud drape, especially in the distal part of the wedge (Fig. 8A to C). The fine-grained grainstone facies is commonly bedded and bioturbated (Fig. 8D). It is also commonly overlain by massive coarse grainstone beds. Wavy grainstone beds and beds with foresets are found in the entire wedge. They generally do not display grading and are moderately bioturbated. Mudstones and wackestones when present are mostly drapes or burrow fills (Fig. 8A, B and E). Packstones are a subordinate facies and often mud lean. Grainstone beds with hummocky and festoon-like structure are found at the exit of the Rotondo Channel. Grainstone beds with grading, top laminations and/or ripples are largely restricted to channel fill successions, for example at Monte Cavallo (Fig. 8F). Thicker grainstone beds in channels can display water escape structures. Grainstones with floating clasts, either intraclasts of the same composition as the surrounding are present throughout the formation. The angular clasts resemble large rip-up clasts (Fig. 8G). Rounded mudstone clasts are also common in such beds, despite the fact that few mudstone and wackestone beds exist in the formation.

The second group is composed of rudstone beds, conglomerates and breccias. The composition of the clasts in rudstones and gravelly breccia beds have two origins. In breccias within the Rotondo Channel and in some thin beds in the basal part of the Orfento Formation the clasts are predominantly from the older platform strata plus reworked clasts from the Orfento Formation (Figs 8H and 10) (Vecsei 1991). All of the other breccias are composed of clasts from the Orfento Formation itself and consist either of large fragments of rudists or as rounded or angular grainstone clasts (Fig. 8I). These intraformational breccias that are internally chaotic and can carry outsized clasts and are reminiscent of high-density turbidity current deposits F2 and F1 of Mutti (1992) or frictional traction carpet facies Tb4 of Postma & Cartigny (2014).

The megabreccias described by Mutti *et al.* (1996) are not included here because they belong lithologically and stratigraphically to the underlying Tre Grotte Formation (Vecsei 1991) that is separated from the Orfento Formation by a significant hiatus (Lampert *et al.*, 1997). In the following the facies of five elements of the prograding wedge of the Orfento Formation are described (Fig. 9).

### *Facies in the Rotondo Channel*

The main facies in the Rotondo Channel between Mte. Focalone and Rotondo are coarse-grained bioclastic grainstone and very coarse rudstone successions with lensoid breccias with clasts from the Orfento Formation. The succession consists of cross-cutting channels of several metres in width that are filled with coarse grainstone to rudstone beds, often displaying coarse tail grading. Towards the mouth of the Rotondo Channel, the succession displays large-scale up to 2 m high cross-bedding that is reminiscent of festoon cross beds. Beds are oriented approximately perpendicular to the channel. Unique to the Rotondo Channel is the occurrence of breccias with platform lithoclasts from the underlying shallow-water carbonates. These breccias are often partly eroded forming relict lenticular convex upward bodies, 10 to 15 m in relief, that are buried by the prograding lobes (Fig. 10) (Vecsei, 1991; Eberli *et al.*, 1993).

The sedimentological succession at the mouth of the Rotondo Channel has been described in detail by Mutti *et al.* (1996) and Vecsei (1998). Here, a thick lobe extends over the platform edge into the northern basin. This first prograding lobe composed of coarse-grained bioclastic grainstone and rudstone is approximately 70 m thick (Fig. 11A). The lobe contains abundant scours of various depth that are filled with amalgamated rudstones, coarse rudist and gastropod debris and intraformational breccias of the Orfento Formation. In the bottomset, current ripples have been observed in bioclastic grainstones (Mutti *et al.*, 1996). Pebbly conglomerate filling scours can be disorganized at the base and become more aligned above (Fig. 11B). Such successions have been described as related to supercritical flow structures (Massari, 2017). Other pebbly conglomerates are horizontally stratified with horizons rich in clasts separated by the grainstone matrix (Fig. 11C) and could be classified as facies F4 using the Mutti classification of high-density turbidity deposits (1992). Such bed composition is indicative of periods of higher and lower deposition from subcritical flows (Postma & Cartigny, 2014)

### *The excavation moat*

Reduced thickness and erosion have been mapped off the approximately 50 to 100 m high and 30° steep escarpment that separated the shallow-water platform from the basin (Figs 1 and 9) (Eberli *et al.*, 1993; Bernoulli *et al.*, 1996; Vecsei *et al.*, 1998). Erosional truncation of the beds within this moat is observed along the eastern flank of the Pesco Falcone to the west of Monte Rotondo (fig. 14 in Eberli *et al.*, 1993). From the moat northward, the strata thickens from 190 m (Monte Cavallo) to 360 m (Maielletta) (Crescenti *et al.*, 1969).

### *The slope channels*

About 2 km north of the Rotondo channel mouth, three channels each 15 to 30 m in thickness are cut into the Orfento Formation at Monte Cavallo (Figs 5 and 6). Their bases mark the sequence boundaries in the Orfento Formation (Eberli *et al.*, 1993; Mutti *et al.*, 1996; Vecsei *et al.*, 1998). The geometry and extent of the channels have a unique characteristic; the channels decrease in thickness downslope and pinch out after about 2 to 3 km. Internally the channels display a 'cut and fill' geometry with a series of erosion horizons between laterally stacked gravelly breccia units (Figs 7 and 12A). The clast composition is almost exclusively from the

Orfento Formation itself consisting of rounded and subangular fine to coarse bioclastic grainstones or of large fragments of rudist debris. The matrix of these intraformational breccias is a bioclastic grainstone to rudstone. The channel fills display an overall fining-upward succession (Mutti *et al.*, 1996). The base of the succession is typically a stack of unorganized pebbly breccias (Fig. 12B) that are overlain by stratified breccia layers within a grainstone matrix (Fig. 12C). The top metres of the channel fills are thick amalgamated grainstone beds that are coarsely graded, sometimes laminated and have water escape structures (Fig. 12D and E). This succession is reminiscent of high-density turbidity current deposit facies F2 to F5 of Mutti (1992).

### *Prograding lobes and clinoforms*

The largest portion of the Orfento Formation is built by vertically stacked and laterally overlapping decametre thick lobes of several hundred metres length. The lobes are generally convex-upward but have complex internal geometries with sigmoidal clinoforms that downlap towards the north in a basinward direction (Figs 13A, 13B and 14). In dip direction, master bedding planes separate the lobes giving the appearance of a continuous uniform thickness, but in strike direction the lobes are thinning (Vecsei, 1991, 1998). The thinner lobes overlie one another vertically, filling depressions and overlapping bedsets as well as locally downcutting beds, making it hard to follow lobes laterally and to determine the exact number of lobes. Some surfaces at the top of the lobes are hardgrounds covered with thin breccias, indicating a pause in sedimentation or a shift of the depocentre laterally or upslope (Vecsei, 1998).

Figure 14 gives a schematic display of the geometry and the facies distribution in the prograding lobes, which consist of variable bundles of sigmoidal clinoforms. The topset of the prograding lobes contain migrating channels, which are cut into parallel beds and are up to 20 m wide and 5 m deep. They are filled with coarse bioclastic (rudist) debris and intraformational breccias eroded from underlying clinoforms. The sediments are transported in these channels to the edge of the lobes and into the foresets. Where the topset is not channelized, it consists of parallel beds with a sharp lower bedding surface, although slight erosional downcutting can be present. In these grainstone beds lenses and intraformational breccias are common. The clasts are often clustered at the base and are typically horizontally aligned but can also occur as patches, randomly distributed within the bed (Fig. 13C). Bed thickness varies from a few centimetres to metres, but 0.2 to 1.0 m thick beds are the most abundant. Some of beds have coarse pebbly conglomerates at the base that grade upward into a coarse grainstone with parallel lamination. Some beds display ripple and foreset laminations at the very top (Fig. 13D).

The foresets consist mostly of grainstone beds and their slope angle varies but can be as high as 25° (Vecsei, 1998). In the more proximal portions, the foreset beds are dominantly sand-sized bioclastic grainstone, while pebble to gravel sized angular and rounded clasts dominate in the lower foresets. Both normal and inverse grading at the base of the foreset is observed in these very coarse beds. These coarse foreset tongues abruptly downlap against thin beds of fine-grained grainstone and packstone facies (Fig. 14).

### *Distal basin (Madonna della Mazza)*

In the more distal position near Pretoro, which is *ca* 10 km basinward of the mouth of the Rotondo Channel and 5 km from the thickest portion of the drift, the lobes form an approximately 300 m thick succession in cliffs that are not accessible. However, a quarry (Madonna della Mazza) is cut into the youngest sequence. 3D GPR data reveals the structural and sedimentological features (Grasmueck *et al.*, 2010; Sekti, 2010; Cilona *et al.*, 2012). The quarry is 64 m long (east–west), and 50 m wide (north–south) with walls rising to a maximum height of about 12 m. Approximately 20 m of the upper part of the Orfento Formation is exposed along the north, west and south quarry walls. The exposed strata are mostly thick-bedded rudist grainstones to rudstones that are interrupted by thin fine-grained wackestone layers marking the bedding surfaces (Fig. 15). The grains are predominantly rudist-bivalve fragments ranging in size from silt to sand. Some other skeletal debris such as echinoderms, sponge spicules, calcispheres and small benthic foraminifera are present in the fine-grained layers. Inter-particle porosity dominates (Fig. 15). The dominant cement is equant to bladed calcite, with subsidiary isopachous cements also present (Sekti, 2010).

In the quarry only four lithofacies units are present: (i) grainstone with lithoclast facies (Fa8); (ii) thin fine-grained wackestone–packstone facies (Fa1); (iii) massive grainstone facies (Fa4); and (iv) bioturbated packstone–grainstone facies (Fa2). The clasts within the breccias and floatstones are all from the Orfento Formation. They are either rounded finer-grained packstone or wackestone pebbles in a coarse grainstone matrix, or angular grainstone intraclasts and small blocks (Fa7) that are up to 15 cm in diameter. Yet, the lithoclastic admixtures are nearly randomly distributed within the beds except that they seem preferentially aligned to the bedding even when they are floating within the bed (Fig. 15). The fine-grained white, chalky layers separate the beds or are reworked as rounded lithoclasts. The reworking of this facies and the other intraformational clasts indicates that cannibalization of the drift deposit is still a common motif 10 km away from the mouth of the Rotondo Channel. The strata in the quarry is slightly thicker towards the present north, indicating the persistence of a divergent geometry of the lobes.

Weathering of the quarry walls makes sedimentary structures and bedding hard to recognize but 3D GPR data acquired in the lower level quarry, covering an area of 26 x 64 m, reveal the small-scale sedimentary geometries in this part of the drift (Figs 16 and 17). The west and north quarry walls are used to correlate the outcrop section into the subsurface GPR data. The fine-grained carbonate layers in the outcrop (labelled 'A' to 'E' in Fig. 15), which are thin, give a high amplitude reflection in the GPR data and thus, can be easily correlated into subsurface GPR data (Fig. 16). The internal structure of the sediment and bedding interfaces create distinctive radar reflection facies. The grainstone with lithoclasts facies (Fa8) produces a high-amplitude continuous reflection GPR facies that is thinning to the north. The thin fine-grained carbonate layer (Fa1) produces a strong and continuous amplitude reflection, while the massive grainstone (Fa4) is correlated into transparent reflection GPR facies (Fig. 17). The bioturbated packstone–grainstone (Fa3) that is exposed in upper portions of the quarry walls is not imaged in the GPR data because it does not occur below the quarry floor (Fig. 16). On the other hand, an inclined reflection GPR facies that forms the base of the GPR cube is not exposed in outcrop (Fig. 16).

The 3D GPR volumes provide accurate information of the depositional geometries of the Orfento Formation. In particular, the sediment transport direction can be assessed. In the flattened volume of the 3D GPR data the progradational packages display a slightly convex upward form, with a thickness of 1.0 to 3.5 m and maximum dip angles of the prograding beds of 15° to 20° (Fig. 18). The prograding packages are bounded by erosional/reactivation surfaces that are bright reflections in the time slice. The internal inclined reflections are straight or sigmoidal and reactivation surfaces cut across some of the prograding beds. The prograding geometry tends to be straight to slightly curved in strike direction but the strike direction of the inclined beds and the transport direction is consistently N18 – 23°E. (Fig. 19).

## DISCUSSION

### Depositional environment

Prior to the deposition of the Orfento Formation, the depositional environments at the Maiella platform margin consisted of the shallow-water Apulian platform and the basin in the north separated by an escarpment (Fig. 1). The prograding bioclastic deposits of the Orfento Formation cover both of these environments. Because of tectonic activity and karstification, the upper Cretaceous platform was at that time an uneven surface with topographic depressions and highs (Sanders, 1994; Rusciadelli & Ricci, 2008). The highs on the platform, which were covered with rudists, were the source for the bioclastic debris in the Orfento Formation. One documented source area was to the east of the Rotondo Channel (Monte Acquaviva, Cima delle Murelle, Valle delle Mandrelle) (Accordi *et al.*, 1987; Sanders 1994). Early workers recognized that the bioclastic grainstones of the Orfento Formation was transported across the neritic environment and far into the adjacent basin (Crescenti *et al.*, 1969). Thus, the depositional environment changed from an escarpment bounded platform to a new system with lower relief, limiting mass gravity flows. The mud-free Orfento Formation was deposited in a high-energy environment that generally associated with shallow water; however, it is overlain by breccias intercalated with limestones containing nannofossils and planktonic foraminifera (Vecsei *et al.*, 1998). As a consequence, assigning the Orfento Formation to a depositional environment has posed a challenge.

Eberli *et al.* (1993) placed the succession into an upper slope environment and interpreted the channels and breccia units as lowstand deposits. Their model implied a sea-level control on the prograding sequences in which the repetitive downward shift of the coarse facies was explained by a long-term lowering of sea-level. However, the lack of exposure horizons in the Orfento Formation in a continuously downstepping system is a problem for this model. Mutti *et al.* (1996) interpreted the vertical facies succession as shoaling from the pelagic to a high energy shoreface environment. When Lampert *et al.* (1997) documented a significant hiatus between the Tre Grotte to the Orfento Formation, it became clear that onset of the high-energy bioclastic deposits of the Orfento Formation is not the result of gradual shoaling. Without the shoaling, a sea-level drop of at least 50 m would be needed to shift the entire depositional system into the basin and would have exposed the source area for the shoreface complexes in the shallow-water area of the platform. Thus, the abrupt transition into the

bioclastic wedge indicates a dramatic change of the depositional motif with drastically increased offbank transport compared to the situation in the underlying platform basin system.

Vecsei (1998) deemed the northward prograding wedge as reminiscent of a tidal delta based on the delta-shaped geometry and the shingled sigmoidal complexes, and explained the lack of bidirectional current indicators and the consistent transport direction to the north, which were measured with alignment of rudists, with a dominant ebb component. Tidal deltas on modern isolated carbonate platforms, however, do not build out into the deep water but are restricted to the platform top where they form characteristic carbonate tidal bars (Rankey & Reeder, 2012). Such carbonate tidal bars are present in the older Cima dell Murelle Formation along the Maiella platform margin (Eberli *et al.*, 1993; Sanders, 1994; Stössel, 1999) but not in the Orfento Formation. One could argue that the Rotondo Channel focused the tidal current similar to what is observed in submarine canyons where tidal currents can reach velocities of 25 to 50 cm/sec (Shepard *et al.*, 1969; Xu *et al.*, 2002). Deep-marine siliciclastic tidal deposits can develop elongate bars that are aligned parallel to the channel axis in the channel-mouth environment and sedimentary features that include sand-mud rhythmites, double mud layers, climbing ripples, mud-draped ripples, alternation of parallel and cross-laminae, sigmoidal cross-bedding with mud drapes, internal erosional surfaces and lenticular and flaser bedding (Shanmugan, 2003). Some sedimentary features at the mouth of the Rotondo Channel in the Maiella are indeed similar; they include sigmoidal clinofolds, mud drapes and lensoid breccias that probably are eroded channel bars (Fig. 10). Yet, other characteristic features of a tidal current regime, like alternations of parallel and cross-laminae and grainstone-mud rhythmites, are missing while abundant deep scouring and reworking of the strata is present that is reminiscent of a unidirectional current regime with changing current strength (Cartigny *et al.*, 2011).

In addition, modern canyons in the Bahamas do not develop deep tidal deltas but only have a thin carbonate fan at their mouth (Mulder *et al.*, 2018), mostly because not enough sediment is supplied to the canyons from the platform top. Tides in the shallow-water carbonate environment form skeletal and non-skeletal (oolitic) tidal bar belts but do not export sand-sized grains into the deep water (Reeder & Rankey, 2008, 2009). Using the modern as an analogue, it is probable that not enough sediment would be exported by tidal currents or storms to build the bioclastic wedge of the Orfento Formation. In tide-dominated siliciclastic deltas, fluvial transport typically brings the necessary material for progradation. In the absence of fluvial transport, another mechanism is needed to bring the sediment from the source area to the edge of the clinofolds.

## **Depositional processes**

The abrupt lithological change from the pelagic succession of the Tre Grotte Formation to the bioclastic wedge of the Orfento Formation reflects a distinct change in depositional processes. In the deep-water Tre Grotte Formation, thick megabreccias and calcareous turbidites, exhibiting classic Bouma sequences, are intercalated into a chalky background sediment (Fig. 5) (Accarie, 1988; Vecsei, 1991; Eberli *et al.*, 1993; Casabianca *et al.*, 2002). In the overlying Orfento Formation the fine-grained chalky background sediment is all but gone. Occasionally, a chalky mudstone to wackestone facies still exists but it is of a different composition with nearly

no age-diagnostic microfossils (foraminifera and coccoliths). The Orfento Formation is a largely mud-free deposit with sedimentary structures that indicate deposition from a variety of subaqueous high-density sediment flows *sensu* Talling *et al.* (2012), or “high-concentrated turbidity current deposits” *sensu* Lowe (1982). Yet, the succession does not fit into any of the existing turbidite models, although many beds display characteristics of the rudite ‘R’ and sandy ‘S’ facies of Lowe (1982) and Massari (1984) or the F2 to F6 facies of Mutti (1992).

The geometry of the depositional wedge with an excavation moat just off the platform margin and the mounded morphology of the wedge in the basin with an apex that is higher than the top of the feeder channel (Figs 5 and 6) is hard to reconcile with a turbidite fan despite the fact that many of the sedimentary structures are reminiscent of high-density sediment flows. Other beds display structures that are associated with hyperpycnal flow, such as gradational bases and tops and inverse followed by normal grading and intersequence erosional contacts (Mulder *et al.*, 2003). Hyperpycnal flow originating from isolated carbonate platforms that lack fluvial transport, can only be achieved by either cascading density currents or channel-focused shallow currents. In addition, other common sedimentary features within the Orfento Formation, such as scours filled with pebble-sized and gravel-sized bioclasts and lithoclasts (Figs 11 and 12), erosive surfaces (Figs 7 and 12), and top-cut-out foresets in clinoform beds are typical features of hydraulic jumps and transitions from supercritical to subcritical flow (Cartigny *et al.*, 2011; Postma & Cartigny, 2014; Postma *et al.*, 2014).

The discovery of a new type of channel-related drift deposit, the delta drift, in the Inner Sea of the Maldives provides a new testable analogue for the deposition of the bioclastic wedge of the Orfento Formation. In the following, the characteristics of the prograding Kardiva delta drifts are briefly described and compared with the Orfento Formation in the Maiella.

### **Comparison with the Kardiva Delta drift**

The bioclastic prograding wedge at the mouth of the Rotondo Channel, which opens into the Umbria-Marche Basin has a modern analogue in the Maldives. In the Maldives, partial drowning formed the southern and northern West-Kardiva Channels. At the exit of these two gateways that connect the Inner Sea of the Maldives with the open Indian ocean, two contourite drifts are deposited (Fig. 20) (Betzler *et al.*, 2016a, b). This channel-related drift type is termed ‘delta drift’ (Lüdmann *et al.*, 2018). Like a river delta, the delta drift is comprised of prograding lobes and connected to a point source, which in this case are the northern and southern West-Kardiva Channels (Fig. 21A). In these delta drifts, the currents transporting the sediment do not follow the contours of the basin but enter the basin perpendicularly through channels formed by the partial drowning of a large continuous platform (Fig. 20; Betzler *et al.*, 2009; Lüdmann *et al.*, 2013, 2018). The currents flowing through the channels carry sediment entrained from the channel floor and shallow-water material shed from the atolls on both sides. Entering the approximately 500 m deep Inner Sea, the currents expand, depositing the sediment load as the flow relaxes in a similar fashion to a river entering a basin. However, in this current-created delta the process is entirely below sea-level (Lüdmann *et al.*, 2018).



### *Size of the Kardiva delta drifts*

The two delta drifts in the Maldives display similar dimensions and thicknesses; they are about 25 km long and 16 to 17 km wide (Fig. 20). The maximum thickness of the northern delta drift is 385 m and approximately 500 m in the southern delta drift (Betzler *et al.*, 2018; Lüdmann *et al.*, 2018). Considering that about one third to one half of the Orfento Formation (150 km<sup>2</sup>) is exposed today, the aerial extent of the prograding wedge of the Orfento Formation is in the same range as the two delta drifts in the Maldives.

### *Architecture of the Kardiva delta drift*

The unique architectural elements of the delta drift include: (i) an overall mounded geometry with an apex that is shallower than the floor of the source channel; (ii) channels cutting downslope that are arranged in a radial pattern; (iii) cyclic steps at the toe of the prograding clinoforms; and (iv) an excavation moat at the transition from the feeder channel to the delta drift (Fig. 21). The large-scale mounded geometry is particularly diagnostic for current-controlled deposition

In the delta drifts of the Maldives, channels cut into the foreset strata of the clinoforms (Fig. 21B and C). They are 0.5 to 1.0 km wide and tens of metres to 150 m deep. The channels are restricted to the steeper middle segment of the clinoforms and fade out basinward. In addition to the channels, smaller gullies that are 100 to 300 m wide and 10 to 15 m deep dissect the steeper, upper part of the prograding lobes (Lüdmann *et al.*, 2018).

At the transition from the steeper to the less inclined clinoforms at the base of the drift, a wavy upward migrating pattern is observed that continues, albeit less developed, throughout the drift (Fig. 21D). These wavy patterns are interpreted as cyclic steps (Lüdmann *et al.*, 2018), which form when the change in slope gradient causes a hydraulic jump where the cascading current decelerates and expands before accelerating again and changing from supercritical to subcritical conditions.

In the Kardiva delta drift an excavation moat forms where the Kardiva Channel enters the Inner Sea (Fig. 21D). In the southern Kardiva delta drift this moat is less developed and is stratigraphically younger (Lüdmann *et al.*, 2018). This excavation moat disappears laterally and is thus different from moats that form along contourite drifts. It is more like a plunge pool at the transition from the channel to the deeper Inner Sea.

### *Sediment facies of the Kardiva delta drift*

The sediments in the Kardiva delta drift consist of coarse-grained facies with abundant shallow-water components in the proximal part of the delta drift and fine-grained facies in the distal portions (Betzler *et al.*, 2018; Lüdmann *et al.*, 2018). Their texture varies from wackestone to rudstone. At Sites U1466 and U1468, the drift successions show a fining-upward trend in the lower part of the depositional package followed by a coarsening-upward trend in its upper part. Wackestones and packstones are bioclastic with benthic and planktonic foraminifera, while the

main components of the grainstones and rudstones are large benthic foraminifera together with echinoid spines, red algae, mollusc fragments, bryozoans, Halimeda plates and aggregate grains (Betzler *et al.*, 2018). In addition, floatstone with angular intraclasts occur in some wackestone units (Lüdmann *et al.*, 2018). Figure 22 shows the stratigraphic column of the underlying platform slope deposits and the delta drift (in yellow) at IODP Site U1468, which is situated at the apex of the delta drift (Fig. 21). In the 390 m thick delta drift, the sedimentary succession displays a fining-upward trend from packstone to wackestone in the basal 200 m and a coarsening-upward trend above (Fig. 22). In the basal 200 m, most sedimentary structures are obliterated by extensive bioturbation. As a result, thick sections of massive packstone to wackestone dominate many cores (Fig. 22B). In the coarse deposits above, mud content decreases significantly and mud-lean packstone and grainstone constitute the finer-grained beds. Rudstone and floatstone beds increase towards the top. In this upper interval, both fining and thinning trends are observed as well as bi-gradational intervals (Betzler *et al.*, 2016a; Lüdmann *et al.* 2018). In addition, several floatstones with angular intraclasts in a wackestone matrix and graded, pebbly conglomerates composed entirely of rounded intraclasts are intercalated in the succession (Figs 22C and 23A). These intraformational floatstone and breccia document the cannibalization of the deposited strata, which is a motif that is very similar to the cannibalization in the Orfento Formation. The top 60 m are coarse bioclastic floatstones to grainstones with abundant large benthic foraminifera that are only slightly abraded (Fig. 22D and E) and, thus, likely to have inhabited the apex of the drift. The entire delta drift is very porous; it has a porosity of around 60% at the top of the drift which decreases to about 40% at the base (Betzler *et al.*, 2016a; Lüdmann *et al.*, 2018). Besides marine cementation, diagenetic features include chert nodules and the development of secondary porosity by dissolution of celestine (Betzler *et al.*, 2016a).

### **Similarities between the Orfento Formation and the delta drifts in the Maldives**

The architecture of the Orfento Formation, with a mounded geometry, an erosional moat just basinward of the Rotondo Channel and sigmoidal clinofolds within the prograding lobes is very similar to the Kardiva delta drifts (Figs 5 and 21). An erosional unconformity forms the top of the drifts in the Maldives and across the Orfento Formation, where it is classified as a supersequence boundary (Vecsei *et al.*, 1998). Within the drift sequence, boundaries are recognized by angular unconformities separating the Kardiva delta drifts into three seismic mega-drift sequences (DS1 to DS3; Fig. 21). These are characterized by onlap and downlap terminations in the proximal position and correlative conformities in a basinward direction (Fig. 3; Lüdmann *et al.*, 2018). In the Orfento Formation four sequences are identified based on similar criteria.

The absence or sparse occurrence of age-diagnostic fossils is a characteristic of the Kardiva delta drift in the Maldives and the Orfento Formation. At the most proximal site (U1466) the bulk of the drift does not contain any age-diagnostic fossils (Betzler *et al.*, 2016). With increasing distance from the channel mouth the fossil content increases and in the most distal site (U1467) a detailed biostratigraphic age model is possible (Betzler *et al.*, 2016). Age-diagnostic fossils are also rare in the Orfento Formation and in the proximal locations the age can only be bracketed by dating the strata below and above. Only in the laterally thinned section

at Pennapiedimonte did a combined biostratigraphy and magnetostratigraphy yield a robust age model.

The sediment facies of the Kardiva delta drifts is richer in mud than the Orfento Formation which is dominated by grainstone and rudstone facies. Yet, several characteristic features are present in both successions. White layers of mud, mud drapes and muddy burrow fills in massive grainstone beds are a common feature in the Orfento Formation and the drift succession in the Maldives (Figs 22C, 22D, 23A and 23B). Pebbly conglomerates of intraclasts are found at both locations. Likewise, breccia layers with angular and rounded intraclasts within grainstone successions are present in both places within the prograding lobes (Fig. 23C and D). The slope channels have not been cored in the Maldives and thus their lithological content is not known. Assuming that the sedimentary facies is the product of a specific sedimentary process, similar processes are operating in the delta drifts of the Maldives and the bioclastic wedge of the Orfento Formation. The increased mud content in the Maldives could indicate a weaker current system in Maldives but could also be related to the increased production of (aragonite) mud in the Cenozoic compared to the calcite production in the Cretaceous.

The similarity between the Maldives and the Maiella also extends to the interpretation. In the Maldives, the late middle Miocene progradation in the delta drift was originally interpreted to be related to the lowering of sea-level during this time (Purdy & Bertram, 1993; Aubert & Droxler, 1996; Belopolsky & Droxler, 2004) before newly acquired seismic data revealed the current control on the deposition (Betzler *et al.*, 2012; Lüdmann *et al.*, 2013). In the Maiella, the slope channels and the shift of the associated facies were also interpreted as a reaction to a long-term lowering of sea-level (Eberli *et al.* 1993; Mutti *et al.*, 1996). The comparison of the sedimentary composition and architecture, however, provides very strong evidence that the bioclastic wedge of the Orfento Formation is a Cretaceous delta drift.

## CONCLUSIONS

The prograding bioclastic wedge of the Orfento Formation fills the Rotondo Channel and forms a convex upward sedimentary body that has many characteristics which are identical or very similar to the delta drifts in the Maldives. These similarities include: (i) a large-scale mounded geometry with offlapping and sigmoidal clinoforms; (ii) a prominent top unconformity and unconformity bounded sequences, downslope disappearing channels filled with coarse intraformational breccias; (iii) sediment sourced from shallower water areas and from the apex of the wedge; (iv) the coarse-grained nature of the deposits; (v) the lack of age-diagnostic fossils in the proximal areas of the wedge; and (vi) a high porosity. In short, the architecture, dimensions and sedimentary geometries of the bioclastic carbonate wedge of the Orfento Formation are in concert with the characteristics of the delta drift in the Maldives.

## Conceptual model of the Maiella Delta drift

The basic requirement for the formation of a carbonate delta drift is a current flowing through a channel that opens to a basin across a knickpoint where current decelerates and releases its sediment load. The sediment is entrained in the current while passing through the channel. The initial depth of the channels, both in the Maiella and the Maldives, is estimated to be tens to a couple of hundred metres. Thus, the currents sweeping through the channels are surface currents. In the Maldives, this current is produced by monsoon winds (Betzler *et al.*, 2016a); in the Maiella it is probably a narrow westward flowing current hugging the southern margin of Tethys (Poulson *et al.*, 1998).

Figure 24 is a schematic display of the bioclastic delta drift in the Maiella and its four sub-environments. A delta drift receives its sediment from a point source, which in this case is the Rotondo Channel, that feeds sediment into an adjacent basin. The feeder channel and the delta are both subaqueous. The topography along which the delta develops is the remnant of the platform escarpment (Fig. 1). The material in the delta drift is predominantly skeletal debris (rudists) from the shallow-water areas along the feeder channel, as well as reworked clasts of previously deposited sediment. The current flowing through the channel transports the sediment but also erodes material from the channel floor.

At the mouth of the channel the current crosses the knickpoint as it flows over the steep escarpment-like margin into the basin. A change from the steep escarpment-like slope to the less inclined slope beyond results in a hydraulic jump, producing an excavation moat where coarse sediment is deposited on the downslope rim and finer-grained sediment spilled over and was further transported downslope. A similar process is envisioned in the creation of the excavation moat at the drop from the Kardiva Channel into the Inner Sea (Fig. 21D). In the Maiella the excavation moat in front of the Rotondo Channel mouth is recorded in reduced thickness of the sections (Figs 5 and 6). The lateral extent of the moat cannot be evaluated in the Maiella but seismic data in the Maldives document that the moat pinches out sideways (Lüdmann *et al.*, 2018). Thus, the origin of the excavation moat is more reminiscent of the formation of a large plunge pool with a flow perpendicular to the moat (Schnyder *et al.*, 2018) and not along contours as is the case in separated drifts (Faugeres *et al.*, 1999; Rebesco *et al.*, 2014).

Interestingly, the reduced sedimentation and erosion at this proximal location persists throughout the deposition of the drift, even after the escarpment topography is buried (Fig. 24). The same persistence of the excavation moat is also observed in both delta drifts in the Maldives (Lüdmann *et al.*, 2018). Thus, the erosion might continue because a mounded topography is created by the initial formation of the moat and the current flowing through the channel hits the stoss side of the mound forcing the current into a subcritical flow and a zone of erosion and subsequent deposition of chaotic breccias and traction carpets as is observed in the proximal part of the wedge at Monte Cavallo (Fig. 12). It is envisioned that, like in a cyclic step, the current then flows over the apex of the delta drift progressively changing into subcritical flow before accelerating on the other side to deposit the inclined beds with the sigmoidal clinofolds.

The slope channels at Monte Cavallo that are filled with various breccias, conglomerates and coarse high-density turbidite deposits start in this hydraulic jump zone (Fig. 12). Their intraformational composition, the abundant erosive surfaces within the breccia beds and the sedimentary structures such as coarse-tail grading, fluid escape structures and conglomerate assemblages are reminiscent of frictional and collisional traction carpets (Postma *et al.*, 2014). Furthermore, the channels thin and pinch out basinward in about 1.5 to 2.0 km, indicating that the erosive power of the current has diminished or that the flow turned from supercritical to subcritical. In the Maldives, the slope channels have not been drilled and thus their composition is not known but their limited extent and the pinch out down drift is similar to the channels in the Maiella delta drift.

The majority of the Maiella delta drift is built by vertically stacked and laterally overlapping lobes. From the mouth of Rotondo Channel to the crest of the drift their tops are eroded, forming a top unconformity (Fig. 1; Vecsei *et al.*, 1998) in a similar way as the top unconformity does in the Maldives (Fig. 21D). The thick lobes display a divergent geometry as the entire delta drift builds into the basin. Internally, the individual decametre thick lobes contain a sigmoidal progradation pattern with channels in the topset supplying the sediment to the foreset and bottomset (Fig. 14). The source of the sediment is debris from shallow-water benthic organisms (mostly rudists and some larger foraminifera), pointing to a source area on the southern platform next to the Rotondo Channel. In the more distal position, skeletal debris from echinoderms and sponges indicate that the delta drift itself was a habitat for these organisms. In the delta drifts of the Maldives, the sediment at the crest of the drift mound is dominated by large benthic foraminifera that probably inhabited the drift before being reworked (Betzler *et al.*, 2016a, Lüdmann *et al.*, 2018). The incorporation of these indigenous fauna into the drift sediments indicates widespread reworking across the entire delta drift.

Reworking or ‘cannibalization’ by currents is a common motif in the depositional processes of the delta drifts. It manifests itself best in the local sourcing of lithoclasts in the small foreset beds in the distal position (Figs 18 and 19), in the abundance of lithoclasts in the sigmoidal clinoforms (Fig. 14), and the intraformational breccias and conglomerates in the slope channel fills. Hardgrounds and gravel lags on master beds separating the lobes and the mud drapes imply that the interruption of deposition is either caused by shifting of the currents or decrease in current strength. It is not clear how much of this fluctuation in current strength is related to sea-level changes as proposed by Vecsei (1998). In other current dominated systems, like in the drifts on the Marion Plateau on the Australian margin, the age of the sequences within the drift is the same as the sea-level produced unconformities in the adjacent platforms, indicating a causal relationship between shifting of the currents and sea-level changes (Eberli *et al.*, 2010).

## Implications

Recognizing that depressions and channels in shallow-water carbonate settings can focus surface currents with the strength to mobilize, transport and deposit coarse-grained sediment to the adjacent basin has implications for carbonate sedimentology and facies models. Similarly, as internal waves can be used to explain cross-bedded grainstone deposits on ramps (Pomar *et al.*, 2012), the focused currents producing channel-related drift deposits invite a new look at

coarse prograding carbonate system in the deeper water around isolated atolls, small platforms and highs, and for sedimentary bodies that hitherto have been described as, for example, neritic shoals, prograding delta lobes, etc.

The Miocene delta drifts in the Maldives and the Upper Cretaceous delta drift in the Maiella share characteristics that can serve as criteria to recognize bioclastic carbonate wedges as delta drifts. These criteria are:

- A large delta-shaped geobody with a slightly mounded geometry and prograding clinoforms downlapping in a basinward direction in a dip section and bi-directionally in a strike section.
- An excavation moat that persists throughout the deposition of the drift at the mouth of the feeder channel.
- A top unconformity from the feeder channel to the apex of the delta drift.
- Potentially high sedimentation rates of largely mud-free bioclastic sediment and reworked clasts.
- A bioclastic composition with very limited biostratigraphic markers in the proximal portion of the delta drift.
- Slope channels that decrease in depth in a basinward direction and eventually pinch out. They are filled with intraformational lithoclastic breccias and coarse grainstone and rudstone.
- Prograding lobes with a complex internal geometry of sigmoidal clinoforms and a channelized topset. The channel fills are pebble to coarse-grained rudstone and finer-grained foresets and bottomsets.

## **ACKNOWLEDGEMENTS**

Financial support for the fieldwork in the Maiella was provided by Swiss National Foundation grants 20-27 457.89 and 20-35907.92 and by funds from industrial associates to the CSL – Center for Carbonate Research. The Maldives research was part of the IODP Expedition 359. We thank the drilling crew, ship's crew and scientific party for all their work. The expedition was funded by the US National Science Foundation (NSF); the European Consortium for Ocean Research Drilling (ECORD); the Ministry of Education, Culture, Sports, Science and Technology, Japan (MEXT); the Ministry of Science and Technology (People's Republic of China); the Korea Institute of Geoscience and Mineral Resources; the Australian Research Council; the New Zealand Institute for Geological and Nuclear Sciences; and the Ministry of Earth Sciences (India). The German Federal Ministry of Education and Research is thanked for funding the seismic surveys (03S0405, 03G0236A). G.P. Eberli received post-cruise funding for this comparative study from Grant OCE-1450528 and industrial associates to the CSL – Center for Carbonate Research. Perceptive comments by the two reviewers Dorrick Stow and Poppe de Boer helped to reorganize and improve the manuscript. We thank Greta MacKenzie for correcting the English and helping us to conform with the Sedimentology guidelines.

## REFERENCES

- Accarie, H.** (1988) Dynamique sédimentaire et structurale au passage platform/bassin. Les faciès Crétacés et Tertiaires: massif de la Maiella (Abruzzi, Italie). *Ecole des Mines de Paris, Mém. Scie. de la Terre*, **5**, 158 pp.
- Accarie, H. and Delamette, M.** (1991) Découverte d'ammonites albiennes dans le massif Apennin de la Maiella (Plateforme Lazio-Abruzzaise; Italie central): précision sur la durée du hiatus bauxitique Médio-Crétacé. *Cret. Res.*, **12**, 81- 90.
- Accarie, H., Beaudoin, B., Cussey, R., Joseph, Ph. and Triboulet, S.** (1986) Dynamique sédimentaire et structurale au passage plateforme/bassin. Les faciès carbonatés crétacés du massif de la Maiella (Abruzzes, Italie). *Mem. Soc. Geol. It.*, **36**, 217-231.
- Accordi, G., Carbone, F., Sirna, G., Catalano, G. and Reali, S.** (1987) Sedimentary events and rudist assemblages of Maiella Mt. (Central Italy): Paleobiogeographic implications. *Geol. Romana*, **26**, 135-147.
- Anselmetti, F. S., Eberli, G.P. and Bernoulli, D.** (1997) Seismic modeling of a carbonate platform margin (Montagna della Maiella, Italy): variations in seismic facies and implications for sequence stratigraphy. In: *Carbonate Seismology* (Eds F.J. Marfurt & A. Palaz), *Soc. Expl. Geol., Geophys. Devel. Series* **6**, 373-406.
- Antonellini, M., Tondi, E., Agosta, F., Aydin, A. and Cello, G.** (2008) Failure modes in deep-water carbonates and their impact for fault development: Majella Mountain, Central Apennines, Italy. *Mar. and Petrol. Geol.*, **25**, 1074-1096
- Aubert, O. and Droxler, A.W.** (1996) Seismic stratigraphy and depositional signatures of the Maldive Carbonate System (Indian Ocean). *Mar. and Petrol. Geol.*, **13**, 503-536.
- Bally, A.** (1954) Geologische Untersuchungen in den SE-Abruzzen. *Ph.D Thesis, Zürich University*, 289 pp.
- Belopolsky, A.V. and Droxler, A.W.** (2004) Seismic expressions of prograding carbonate bank margins: middle Miocene, Maldives, Indian Ocean. In: *Seismic Imaging of Carbonate Reservoirs and Systems* (Eds G.P. Eberli, J.L. Masferro & J.F. Sarg), *AAPG Mem.*, **81**, 267–290.
- Bernoulli, D.** (1972) North Atlantic and Mediterranean Mesozoic facies, a comparison. In. *Initial Reports of the Deep Sea Drilling Project*, Hollister, C.D., J.I. Ewing, *et al.*, Washington, D.C., U.S. Government Printing Office: **11**, 801-871.
- Bernoulli, D.** (2001) Mesozoic-Tertiary carbonate platforms, slopes and basins of the external Apennines and Sicily. In: *Anatomy of an Orogen: The Apennines and Adjacent Mediterranean Basins* (Eds F. Vai and P. Martini), pp. 307–325. Dordrecht, The Netherlands, Springer. Available at: doi:10.1007/978-94-015-9829-3\_18.
- Bernoulli, D., Anselmetti, F.S., Eberli, G.P., Mutti, M., Pignatti, J.S., Sanders, D.G.K. and Vecsei, A.** (1996) Montagna della Maiella: the sedimentary and sequential evolution of a

- Bahamian-type carbonate platform of the South-Tethyan continental margin. *Mem. Soc. Geol. Ital.*, **51**, 7-12.
- Betzler, C.G., Eberli, G.P., Alvarez Zarikian, C.A. and the IODP Expedition 359 Scientists** (2016a) Expedition 359 Preliminary Report: *Maldives Monsoon and Sea Level*. *International Ocean Discovery Program*. Available at: <http://dx.doi.org/10.14379/iodp.pr.359.2016>
- Betzler, C.G., Eberli, G.P., Alvarez Zarikian, C.A. and the IODP Expedition 359 Scientists** (2016b) The Abrupt Onset of the Modern South Asian Monsoon Winds. *Nature Sci. Reports* **6**, **29838**. Available at: <https://www.nature.com/articles/srep29838>
- Betzler, C.G., Eberli, G.P., Lüdmann, T., Reolid, J., Kroon, D., Reijmer, J.J.G., Swart, P.K., Wright, J.D., Young, J.R., Alvarez-Zarikian, C.A., Alonso-García, M., Bialik, O.M., Blättler, C.L., Guo, J.A., Haffen, S., Horozal, S., Inoue, M., Jovane, L., Lanci, L., Laya, J.C., Ling A.H.M., Nakakuni, M., Nath, B.N., Niino, K., Petruny, L.M., Pratiwi, S.D., Slagle, A.L., Sloss, C.R., Su, X. and Yao, Z.** (2018) Refinement of Miocene sea level and monsoon events from the sedimentary archive of the Maldives (Indian Ocean). *Prog. Earth and Planet. Sci.*, **5**, 5. Available at: <https://doi.org/10.1186/s40645-018-0165-x>
- Betzler, C., Fürstenau, J., Lüdmann, T., Hübscher, C., Lindhorst, S., Paul, A., Reimer, J. and Droxler, A.W.** (2012) Sea-level and ocean-current control on carbonate platform growth, Maldives, Indian Ocean. *Basin Res.*, **24**, 1-15.
- Betzler, C., Hübscher, C., Lindhorst, S., Reijmer, J.J.G., Römer, M., Droxler, A., Fürstenau, J. and Lüdmann, T.** (2009) Monsoon-Induced Partial Carbonate Platform Drowning (Maldives, Indian Ocean). *Geology* **37**, 867-870.
- Betzler, C., Reijmer J. J. G., Bernet, K., Eberli, G. P. and Anselmetti, F. S.** (1999) Sedimentary patterns and geometries of the Bahamian outer carbonate ramp (Miocene and lower Pliocene, Great Bahama Bank). *Sedimentology*, **46**, 1127-1145.
- Brandano, M., Tomasetti, L., Saedella, R. and Tinelli, C.** (2016) Progressive deterioration of trophic conditions in a carbonate ramp environment: the *Lithothamnion* limestone, Majella Mountain (Tortonian–early Messinian, Central Apennines, Italy). *PALAIOS*, **31**, 125–140,
- Cartigny, M.J.B., Postma, G., van den Berg, J.H. and Mastbergen, D.** (2011) A comparative study of sediment waves and cyclic steps based on geometries, internal structures and numerical modelling. *Mar. Geol.* **280**, 40–56.
- Casabianca, D., Boscence, D. and Beckett, D.** (2002) Reservoir potential of Cretaceous platform-margin breccias, Central Italian Apennines. *J. Petr. Geol.*, **25**, 179-202.
- Catenacci, V.** (1974) Note illustrative della Carta Geologica d'Italia. Foglio 147, Lanciano. *Serv. Geol. d'Ital.*, Roma, 87 pp.
- Cilona, A., Baud, P., Tondi, E., Agosta, F., Vinciguerra, S., Rustichelli, A. and Spiers, C. J.** (2012). Deformation bands in porous carbonate grainstones: Field and laboratory observations. *J. Struct. Geol.*, **45**, 137-15



- Crescenti, U., Crostella, A., Donzelli, G. and Raffi, G.** (1969) Stratigrafia della serie calcarea dal Lias al Miocene nella regione Marchigiano-Abruzzese (Parte II - Litostratigrafia, biostratigrafia, paleogeografia). *Mem. Soc. Geol. Ital.*, **8**, 343-420.
- Eberli, G.P.** (2013) The uncertainties involved in extracting amplitude and frequency of orbitally driven sea-level fluctuations from shallow-water carbonate cycles. *Sedimentology*, **60**, 64-84.
- Eberli, G.P., Anselmetti, F.S., Betzler, C., Van Konijnenburg, J.-H. and Bernoulli, D.** (2004) Carbonate platform to basin transition on seismic data and in outcrop – Great Bahama Bank and the Maiella platform, Italy. In: *Seismic Imaging of Carbonate Reservoirs and Systems* (Eds G.P. Eberli, J.L. Massafello and J.F. Sarg), *AAPG Mem.*, **81**, 207-250.
- Eberli, G.P., Anselmetti, F.S., Isern, A.R. and Delius, H.** (2010) Timing of sea-level changes and currents along Miocene platforms on the Marion Plateau. In: *Cenozoic Carbonate Systems of Australasia*. (Eds W.A. Morgan, A.D. George, P.M. Harris, J.A. Kupecz and J.F. Sarg), *SEPM Spec. Publ.* **95**, 219-242.
- Eberli, G.P., Bernoulli, D., Sanders, D. and Vecsei, A.** (1993) From aggradation to progradation: the Maiella platform margin (Abruzzi, Italy). In: *Cretaceous Carbonate Platforms* (Eds J.T. Simo, R.W. Scott and J.-P. Masse), *AAPG Mem.*, **56**, 213-232.
- Faugères, J.C., Stow, D.A.V., Imbert, P. and Viana, A.** (1999) Seismic features diagnostic of contourite drifts. *Mar. Geol.*, **162**, 1-38.
- Föllmi, K.B. and Delamette, M.** (1991) Model simulation of mid-Cretaceous ocean circulation, *Science*, **251**, 94, 1991.
- Ghisetti, F. and Vezzani, L.** (2002), Normal faulting, extension and uplift in the outer thrust belt of the central Apennines (Italy): Role of the Caramanico fault. *Basin Res.*, **14**, 225 – 236.
- Grasmueck, M., Marchesini, P., Eberli G.P., Zeller, M. and Van Dam, R.L.** (2010) 4D GPR tracking of water infiltration in fractured high-porosity limestone. *Proc. XIII Int. Conf. G.P.R.*, Lecce, 2010, 563-569. Available at: doi: 10.1109/ICGPR.2010.5550069
- Iannace, A. and Zamparelli, V.** (2002) Upper Triassic platform margin biofacies and the paleogeography of Southern Apennines. *Palaeogeog., Palaeoclim., Palaeoecol.*, **179**, 1-18.
- Lampert, S.A., Lowrie, W., Hirt, A.M., Bernoulli, D. and Mutti, M.** (1997) Magnetic and sequence stratigraphy of redeposited Upper Cretaceous limestones in the Montagna della Majella, Abruzzi, Italy. *Earth and Planetary Science Letters* **150**, 79–83.
- Lowe, D.R.** (1982) Sediment gravity flows. 2. Depositional models with special reference to high density turbidity currents. *J. Sed. Pet.*, **52**, 279–298.
- Lüdmann, T., Betzler, C., Eberli, G.P., Reolid, J. and the IODP Expedition 359 Scientists** (2018) Carbonate delta drift: a new sediment drift type. *Mar. Geol.*, **401**, 98-111.
- Lüdmann, T., Kalvelage, C., Betzler, C., Fürstenau, J. and Hübscher, C.** (2013) The Maldives, a giant isolated carbonate platform dominated by bottom currents. *Mar. Petrol. Geol.*, **43**, 326-340.

- Marchesini, P. and Grasmueck, M.** (2015) The impact of high-density spatial sampling versus antenna orientation on 3D GPR fracture imaging. *Near Surf. Geoph.*, **13**, 197-207.
- Massari, F.** (1984) Resedimented conglomerates of a Miocene fan-delta complex, Southern Alps, Italy. *Can. Soc. Petrol. Geol. Mem.*, **10**, 259–278.
- Massari, F.** (2017) Supercritical-flow structures (backset-bedded sets and sediment waves) on high-gradient clinoform systems influenced by shallow-marine hydrodynamics. *Sed. Geol.*, **360**, 73-95
- Maura, I. A.** (2013) Reservoir Potential of Cretaceous - Tertiary Redeposited Deep-water Carbonates: A Core and Outcrop Study in the Apennines and the Adriatic Sea, Italy. *Open Access Theses*, Paper 454.
- Morsilli, M., Bosellini, A. and Rusciadelli, G.** (2004) The Apulia carbonate platform margin and slope, Late Jurassic to Eocene of the Maiella and Gargano Promontory. Physical Stratigraphy and Architecture, in 32nd International Geological Congress, Agenzia per la protezione dell'ambiente e per i servizi tecnici, Florence, Italy, August 20–28, 2004, pp. 1–44.
- Morsilli, M., Rusciadelli, G. and Bosellini, A.** (2002) Large-scale gravity-driven structures: control on margin architecture and related deposits of a Cretaceous Carbonate Platform (Montagna della Maiella, Central Apennines, Italy). *Boll. Soc. Geol. It.*, **1**, 619-628,
- Mostardini, F. and S. Merlini** (1986) Appennino Centro Meridionale, Sezioni geologiche e proposta di modello strutturale. *76 Congresso, Societa' Geologica Italiana*, Roma, 1–46.
- Mulder, T., Gilletta, H., Hanquiez, V., Reijmer, J.J.G., Droxler, A.W., Recouvreur, A., Fabregas, N., Cavailhes, T., Fauquembergue, K., Blank, D.G., Guiastrennec, L., Seibert, C., Bashah, S., Bujan, S., Ducassou, E., Principaud, M., Conesa, G., Le Goff, J., Ragusa, J., Busson, J. and Borgomano, J.** (2019) Into the deep: A coarse-grained carbonate turbidite valley and canyon in ultra-deep carbonate setting. *Mar. Geol.*, **407**, 316-333.
- Mulder, T., Syvitski, J.P.M., Migneon, S., Faugeres, J.C. and Savoye, B.** (2003) Marine hyperpycnal flows: initiation, behaviour, and related deposits. A review. *Mar. Petrol. Geol.*, **20**, 861–882.
- Mutti, E.** (1992) Turbidite Sandstones. Istituto di Geologia Universita' di Parma & AGIP, San Donato Milanese, 275 pp.
- Mutti, M.** (1995) Porosity development and diagenesis in the Orfento Supersequence and its bounding unconformities (Upper Cretaceous, Maiella Mountains, Italy). In: *Unconformity and Porosity in Carbonate Strata* (Eds D.A. Budd, A.H. Saller, P.M. Harris) *AAPG Memoir* 63, 141-158.
- Mutti, M., Bernoulli, D., Eberli, G.P. and Vecsei, A.** (1996) Facies associations and timing of progradation with respect to sea level cycles in an Upper Cretaceous platform margin (Orfento Supersequence, Maiella, Italy). *J. Sediment. Res.*, **66**, 781-799.

- Patacca E. and Scandone P.** (2007) Geology of the Southern Apennines. *Boll. Soc. Geol. It., Spec. Issue, 7*, 75-119.
- Patacca, E., Scandone, P., Di Luzio, E., Cavinato, G.P. and Parotto, M.** (2008) Structural architecture of the central Apennines: Interpretation of the CROP 11 seismic profile from the Adriatic coast to the orographic divide. *Tectonics*, **27**, TC3006. Available at: doi:10.1029/2005TC001917
- Pomar, L., Morsilli, M., Hallock, P. and Bádenas, B.** (2012) Internal waves, an under-explored source of turbulence events in the sedimentary record. *Earth-Science Reviews* **111**, 56–81.
- Poulson C.J., Seidov, D., Barron, E.J. and Peterson, W.H.** (1998) The impact of paleogeographic evolution on the surface oceanic circulation and the marine environment within the mid-Cretaceous Tethys. *Paleoceanography* **13**, 546-559.
- Postma, G. and Cartigny, M.J.** (2014) Supercritical and subcritical turbidity currents and their deposits—A synthesis. *Geology*, **42**, 987-990.
- Postma, G., Kleverlaan, K. and Cartigny, M.J.** (2014) Recognition of cyclic steps in sandy and gravelly turbidite sequences, and consequences for the Bouma facies model. *Sedimentology*, **62**, 2268-2290.
- Purdy, E. and Bertram, G.T.** (1993) Carbonate concepts from the Maldives, Indian Ocean. *AAPG Stud. Geol.*, **34**, **56 pp.**
- Rankey, E.C. and Reeder S.L.** (2012) Tidal sands of the Bahamian archipelago. In: *Principles of Tidal Sedimentology* (Eds R.A. Davis Jr. and R.W. Dalrymple), pp. 537-565. Springer-Verlag, Berlin.
- Rebesco, M., Hernández-Molina, F.J., Van Rooij, D. and Wåhlin, A.** (2014) Contourites and associated sediments controlled by deep-water circulation processes: State-of-the-art and future considerations. *Mar. Geol.* **352**, 111-154.
- Reeder, S.L. and Rankey, E.C.** (2008) Interactions between tidal flows and ooid shoals, northern Bahamas. *Jour. Sed. Res.* **78**, 175–186
- Reeder, S.L. and Rankey, E.C.** (2009) Controls on morphology and sedimentology of carbonate tidal deltas, Abacos, Bahamas. *Mar. Geol.* **267**, 141–155
- Rusciadelli, G.** (2005) Provenance of Upper Pliocene conglomerates of the Mutignano Formation (Abruzzo, Italy): Implications for unraveling the uplift history of the Central Apennines external zones. *Boll. Soc. Geol. Ital.*, **124**, 645-659.
- Rusciadelli, G. and Di Simone, S.** (2007) Differential compaction as a control on depositional architectures across the Maiella carbonate platform margin (central Apennines, Italy). *Sed. Geol.*, **196**, 133-145.
- Rusciadelli, G. and Ricci, C.** (2008) New geological constraints for the extension of the northern Apulia platform margin west of the Maiella Mt. (Central Apennines, Italy). *Boll. Soc. Geol. Ital.*, **127**, 375-387.

- Rusciadelli, G., Sciarra, N. and Mangifesta, M.** (2003) 2D modelling of large-scale platform margin collapses along an ancient carbonate platform edge (Maiella Mt., Central Apennines, Italy): Geological model and conceptual framework. *Palaeog., Palaeocl., Palaeoec.*, **200**, 245-262.
- Sanders, D.G.K.** (1994) Carbonate platform growth and erosion: the Cretaceous to Tertiary of Montagna della Maiella, Italy. *PhD thesis no. 10800, Eidg. Techn. Hochschule Zürich*. 122 pp. + appendices.
- Schnyder, J.S.D., Eberli, G.P., Betzler, C., Schiebel, L., Lindhorst, S., Wunsch, M., Mulder, T. and Ducassou, E.** (2018) Morphometric analysis of plunge pools and sediment wave fields along western Great Bahama Bank. *Mar. Geol.*, **397**, 15-28.
- Sekti, R.P.** (2010) 3-D stratigraphy and fracture characterization in Late Cretaceous carbonates (Madonna della Mazza, Italy). *Unpubl. MSc Thesis, University of Miami*, Coral Gables, Florida, 105 pp.
- Shanmugam, G.** (2003) Deep-marine tidal bottom currents and their reworked sands in modern and ancient submarine canyons. *Marine and Petroleum Geology* **20**, 471–491.
- Shepard, F. P., Dill, R. F. and Von Rad, U.** (1969). Physiography and sedimentary processes of La Jolla Submarine Fan and Fan-Valley, California. *AAPG Bulletin*, **53**, 39–420.
- Stössel, I.** (1999) Rudists and carbonate platform evolution: The late Cretaceous Maiella carbonate platform margin, Abruzzi, Italy. *Mem. Sci. Geol.*, **51**, 333-413.
- Talling, P.J., Masson, D.G., Sumner, E.J. and Malgesini, G.** (2012) Subaqueous sediment density flows: depositional processes and deposit types. *Sedimentology*, **59**, 1937–2003.
- Vecsei, A.** (1991) Aggradation und Progradation eines Karbonatplattform-Randes: Kreide bis Mittleres Tertiär der Montagna della Maiella, Abruzzen. *Mitt. Geol. Inst. Eidg. Tech. Hochschule Zürich*, **294**, 169 pp.
- Vecsei, A.** (1998) Bioclastic sediment lobes on a supply dominated Upper Cretaceous carbonate platform, Montagna della Maiella. *Sedimentology*, **45**, 473-487.
- Vecsei, A. and Moussavian, E.** (1997) Paleocene reefs in the Maiella platform margin, Italy: An example of the effects of the Cretaceous/Tertiary boundary events on reefs and carbonate platforms. *Facies*, **36**, 123-140.
- Vecsei, A. and Sanders, D.G.K.** (1997) Sea-level highstand and lowstand shedding related to shelf margin aggradation and emersion, Upper Eocene-Oligocene of Maiella carbonate platform, Italy. *Sediment. Geol.*, **112**, 219-234.
- Vecsei, A., Sanders, D., Bernoulli, D., Eberli, G.P. and Pignatti, J.S.** (1998) Sequence stratigraphy and evolution of the Maiella carbonate platform margin, Cretaceous to Miocene, Italy. In: *The Mesozoic and Cenozoic Sequence Stratigraphy of European Basins* (Eds P.-C. De Graciansky, J. Hardenbol, T. Jacquin and P.R. Vail), *SEPM Spec. Publ.* **60**, 53 -74.
- Vitale, S. and Ciarcia, S.** (2013). Tectono-stratigraphic and kinematic evolution of the southern Apennines/ Calabria–Peloritani Terrane system (Italy). *Tectonophysics*, **583**, 164–182.

- Vitale, S., Amore, O.F., Ciarcia, S., Fedele, L., Grifa, C., Prinzi, E.P. and Tavani, S. (2017)** Structural, stratigraphic, and petrological clues for a Cretaceous–Paleogene abortive rift in the southern Adria domain (southern Apennines, Italy). *Geol. Jour.*, 53, 660–681. Available at: DOI 10.1002/gj.2919
- Xu, J. P., Noble, M., Eittreim, S. L., Rosenfeld, L. K., Schwing, F. B. and Pilskaln, C. H. (2002).** Distribution and transport of suspended particulate matter in Monterey Canyon, California. *Mar. Geol.*, **181**, 215–234.
- Zappaterra, E. (1994)** Source-rock distribution model of the Periadriatic Region. *AAPG Bull.* **78**, 333–354.

## FIGURE CAPTIONS

Fig. 1. (A) Schematic stratigraphic relationship across the Maiella platform margin displaying the lower and upper Cretaceous platform and the adjacent basinal deposits of the Tre Grotte Formation. The Upper Campanian to Upper Maastrichtian (Cmp–Maa) Orfento Formation is a thick bioclastic unit that mantles the platform margin morphology and is the focus of this study. ‘0’ to ‘6’ are supersequences as defined by Vecsei (1991) and Vecsei *et al.* (1998). Formations are from Crescenti *et al.* (1969) and redefined by Vecsei (1991). (B) Chronostratigraphic diagram of the Maiella platform margin. Many formations consist of shallow-water platform facies (brick signature), or basinal and slope facies units that are part of one of several supersequences (shaded or white). Two formations coincide with supersequences (Orfento Formation SS 2, Bolognano Formation SS 6).

Fig. 2. (A) Location map of the Maiella platform margin and its present position on the Maiella – Apulia platform. Basinal and slope successions separate this platform from the Lazio – Abruzzi platform. Pelagic sediments in the Umbria–Marche basin are to the north (modified from Eberli *et al.*, 1993). (B) Simplified geological map of the northern portion of the Maiella anticline. A–B indicates approximate location of the schematic stratigraphic profile shown in Fig. 1A. Stippled line is the trace of the cross-section in Fig. 5. (modified from Brandano *et al.*, 2016).

Fig. 3. Three-dimensional reconstruction of the Maiella platform margin during the Late Cretaceous with an escarpment and the ‘drowning seaway’ here called the Rotondo Channel. Modified from Rusciadelli *et al.*, 2003.

Fig. 4. (A) Photograph of the boundary between the Tre Grotte Formation and the Orfento Formation in the Valle Tre Grotte west of Pennapedimonte. The Tre Grotte Formation consists of calcareous turbidites and megabreccias in fine-grained scaglia (periplatform ooze). It is overlain by the coarse-grained bioclastic deposits of the Orfento Formation. A hiatus that spans most of the *G. venriculosa* zone exists between the two formations. Arrows labelled ‘b’ and ‘c’ point to the location of the close-ups in (B) and (C). (B) Base of the megabreccia with platform lithoclasts within the Tre Grotte Formation. Backpack for scale. (C) Example of the thin-bedded calcareous turbidites ( $T_b$  and  $T_c$ ) in the scaglia of the Tre Grotte Formation. (D) Scanning electron microscopy (SEM) picture of the pelagic background sediment with abundant coccoliths of the Tre Grotte Formation. Stratigraphic ages from Lampert *et al.* (1997).

Fig. 5. Reconstruction of the architecture of the Orfento Formation. The deposits form a mounded delta-shaped sedimentary body that has its apex (360 m) at the Santo Spirito location and thins to the east and west as well as to the north. 150 km<sup>2</sup> (15 x 10 km) are exposed in the Maiella anticline and constitute about a third of the entire sedimentary body. An approximately 200 m deep feeder channel (Rotondo Channel) is situated between Monte Rotondo and the Cima delle Murelle. Section Focalone north is located at the exit of the channel.

Fig. 6. South–north cross-section displaying the thickness variations of the bioclastic wedge of the Orfento Formation. The wedge has a mounded morphology with the thickest portion at Santo Spirito, forming an apex that is higher than the top of the feeder channel coming from the platform where the thickness is reduced. The base of the sections is placed on a slope with a 5° slope angle. All sections used are bounded at the base by the Tre Grotte Formation and on the top by the Tertiary Santo Spirito Formation. Sections are taken and redrawn from Vecsei (1991).

Fig. 7. Photograph across the Orfento Valley displaying about 3.5 km of the Orfento Formation overlaying the Tre Grotte Formation that onlaps the escarpment of the Upper Cretaceous platform. The Orfento Formation is also a supersequence bounded by two supersequence boundaries (SSB). The basal SSB is mostly conformable, while the top SSB is an erosional unconformity that removes about 50 m of the Orfento Formation at Monte Belvedere, which is approximately 300 m thick at this location. The slope channels at Monte Cavallo pinch out in a downslope direction (to the left). MB = megabreccias.

Fig. 8. Examples of facies within the Orfento Formation. (A) Fa1; mud layer offset by a small fault (Madonna della Mazza). (B) Fa3; grainstone with burrows filled by white mud (Mte. Focalone north). (C) Fa3; photomicrograph of bioclastic grainstone (Pennapiedimonte). (D) Fa2; fine-grained bioclastic grainstone with parallel bedding and bioturbation (Mte. Focalone north). (E) Top of a pebbly conglomerate with rounded fine-grained clasts from the Orfento Formation (Fa9) overlain by fine-grained bioclastic grainstones with white wackestone layers (Fa2, Fa3) that are truncated by the overlying layer (upward pointing arrows mark the truncation surface) layer with foresets (left pointing arrows) followed by a fine grainstone with small white mudstone lithoclasts (Fa8) (base indicated by down pointing arrows) (Santa Spirito). (F) Fa7; top of a grainstone bed with parallel laminations and ripples. Coin is 2 cm in diameter (Monte Cavallo). (G) Fa8; grainstone with large angular intraclasts (Madonna della Mazza). (H) Fa9; badly sorted pebbly conglomerate of clasts reworked from the Orfento Formation (Monte Cavallo). (I) Fa10; scour filled with chaotic breccia with platform lithoclasts and reworked clasts of Orfento Formation (Rotondo Channel) (arrows mark the base of the scour).

Fig. 9. Schematic display of the bioclastic wedge of the Orfento Formation with the different environments and their facies and bedforms.

Fig. 10. Photograph of a convex-upward lenticular breccia that is onlapped and covered by the prograding lobe at Mte. Focalone. Image on the right is a close-up of the breccia displaying the angular clasts and the lack of matrix. Hammer in circle is 32 cm long.

Fig. 11. Prograding lobe at Mte. Focalone. (A) Three packages (1 to 3) of the basal prograding lobe of the Orfento Formation covering the platform edge with fine grainstone base (fB) and an overlying thick, cliff-forming foreset. (B) Close-up of a 3 m deep scour within the prograding lobe that is filled with breccia and coarse grainstone. (C) Close-up of first package with a

whitish fine-grained base (fB) and an approximately 20 m thick succession of coarse grainstone to rudstone (cF) with breccia layers (B).

Fig. 12. Channel architecture and sedimentary fill at Monte Cavallo. (A) The uppermost channel consists of a laterally stacked scour and fill succession. The fills are typically fining upward from breccias at the base to coarse bioclastic rudstone/grainstone on top. (B) Close-up of the basal conglomerate (below stippled line in (A) displaying the rounded nature of the pebble-sized lithoclasts that are reworked from the grainstone facies in the Orfento Formation. Coin is 2 cm in diameter. (C) Amalgamated coarsely graded bed with traction carpets. The components of the traction carpets are exclusively rounded lithoclasts of the Orfento Formation. (D) Intersequence erosive contact between laminated grainstone and overlying bioclastic floatstone. Hammer is 32 cm. (E) Fluid escape structure in graded and laminated bed. Hammer is 55 cm.

Fig. 13. Example of the architecture and sedimentary structures of the prograding clinofolds beds in the valley of Santo Spirito. (A) Thick composite bed displaying the sigmoidal foreset beds (fs) that downlap in the bottomset (bs) onto a hardground. The thick-bedded topset (ts) slightly truncates the foreset beds. (B) Base of approximately 20 m thick composite bed with a thick foreset and thin bottomset that tangentially downlaps onto the underlying topset. (C) Brown packstone and fine grainstone beds with dispersed clasts of reworked, white wackestone-packstone, a pebbly conglomerate layer, and thin laminations. (D) Close-up of a coarse-tail graded turbidite with lithoclasts at the base and a sharp grain-size boundary to the overlying laminated interval with ripples on top. Coin is 2 cm in diameter in the underlying topset.

Fig. 14. Schematic display of the geometry and grain distribution of the prograding lobes. Each lobe is a composite bed of 10 to 20 m thickness in which the sigmoidal foresets downlap towards the bottomset. The topset contains up to 20 m wide and 5 m deep channels filled with breccias composed of intraformational lithoclasts and coarse bioclastic debris. Sediment is transported to clinofolds through these channels. In the sigmoidal foresets the coarse (breccia) material accumulates near the base mostly displaying normal grading. The bottomset is generally finer grained but layers and lenses of intraformational breccias/conglomerates are present. (modified from Vecsei, 1998).

Fig. 15. Lithological section, outcrop photographs and thin section photomicrographs of the Orfento Formation in the quarry at Madonna dell Mazza approximately 10 km basinward of the mouth of the Rotondo Channel. Photographs display the four facies (Fa1, Fa3, Fa4 and Fa8) observed in the quarry walls. Thin white wackestone layers (Fa1) mark bedding surfaces in the grainstone facies. Reworking of these finer-grained layers and grainstone lithoclasts is common. Photomicrographs reveal well-sorted skeletal debris in the coarser grainstone (Fa3 and Fa8) and the admixture of mud in the finer-grained packstone to grainstone (Fa3). All lithologies have over 30% porosity.

Fig. 16. Correlation of outcrop with ground penetrating data (GPR) in the Madonna dell Mazza quarry's west wall. (A) Lithological section. (B) Quarry wall with bedding surfaces ('A' to 'F') in various colours; red lines are fractures. (C) Close-up of quarry wall displaying the scattered nature of light rounded lithoclasts in the grainstone as well as the thin white wackestone layers

used for correlation. (D) GPR inline parallel to the quarry wall with the horizons used for correlation.

Fig. 17. Three-dimensional view of the GPR volume with GPR facies with the Madonna della Mazza quarry walls as a backdrop. The inclined reflection radar facies with a series of prograding foreset packages with *ca* 1.0 to 3.5 m thickness is not exposed in outcrop. The parallel continuous radar facies that correlates to the grainstone with lithoclasts facies in outcrop is slightly decreasing in thickness to the north. The transparent radar facies correlates to the massive grainstone facies in outcrop.

Fig. 18. Inline through the flattened volume displaying the depositional geometry of the inclined reflection radar facies. The 1 to 3 m thick prograding beds show variability in the foreset dips with maximum angles between 15 to 20°. High amplitude reflections mark the boundaries of the bedsets and resemble reactivation surfaces. Madonna della Mazza quarry.

Fig. 19. Cut into flattened 3D volume, displaying the dip and direction of the prograding bedsets in the Madonna della Mazza quarry. The maximum dip in all bedsets is 15 to 20° and the direction of progradation is 15 to 18° north.

Fig. 20. Location and dimensions of the delta drifts in the Maldives. (A) Location of the Maldives, more than 1000 km long double string of atolls, within the Indian Ocean. (B) Atoll configuration with the location of the Kardiva Channel and the study area. (C) Late Miocene sea floor topography around the Guidhoo Atoll. Two channels, the precursors of the modern Kardiva Channel, cut across the western platform rim, connecting the Indian Ocean to the west with the 500 m deep Inner Sea. Currents flowing through these channels drop their sediment load at the mouth of the channels and form two delta drifts.

Fig. 21. (A) Sketch of the delta drift in plain view and in strike and dip view. (B) Close-up of slope channels – stippled box in (C). These channels cut into the underlying strata but pinch out downslope. (C) Seismic dip line across the northern delta drift with the location of the IODP Sites. (D) Interpreted seismic line with a grey mask over the delta drift, the top unconformity is the wavy red line and the seismic sequences are various other colours. Wavy reflection pattern at the base is interpreted as cyclic steps. Sigmoidal clinoforms construct the delta drift. An excavation moat forms off the knickpoint of the platform in the adjacent basin (modified from Lüdmann *et al.*, 2018). (E) Synthetic seismic section from the Cretaceous Maiella platform into the Umbria-Marche Basin. The bioclastic wedge of the Orfento Formation is coloured green (modified from Anselmetti *et al.*, 1997).

Fig. 22. Lithological section and core photographs at IODP Site U-1468 located at the apex of the delta drift. (A) Lithological section with drift strata in yellow. (B) Massive packstone facies that is representative for the basal portion of the drift deposit. (C) Graded rudstone with rounded lithoclasts at the base transitioning into skeletal debris. A 2 cm white layer of fine-grained packstone is partly eroded by the rudstone. (D) Foraminiferal rudstone with thin white intercalations of packstone and a coarsening-fining upward trend between the top two layers. (E) Close-up of the rudstone [blue box in (D)] consisting predominantly of large benthic foraminifera.

Fig. 23. Examples of similar facies in the Maiella and Maldives delta drift. (A) Core section from IODP Site U1468 showing a bioturbated grainstone with burrows filled with white fine-grained



sediment (white arrows). (B) Bioclastic grainstone bed from the Maiella (Mte. Focalone) with heavily bioturbated top and burrow fills of white wackestone (white arrows) and a bioturbated white wackestone layer near the bottom of the bed. Coin is 2 cm in diameter. (C) Breccia bed with coarse-tail grading of angular to sub-rounded clasts in core 27 at IODP Site U1468. (D) White angular to rounded clasts at the base of a bed with laminated top; Santo Spirito valley, Maiella.

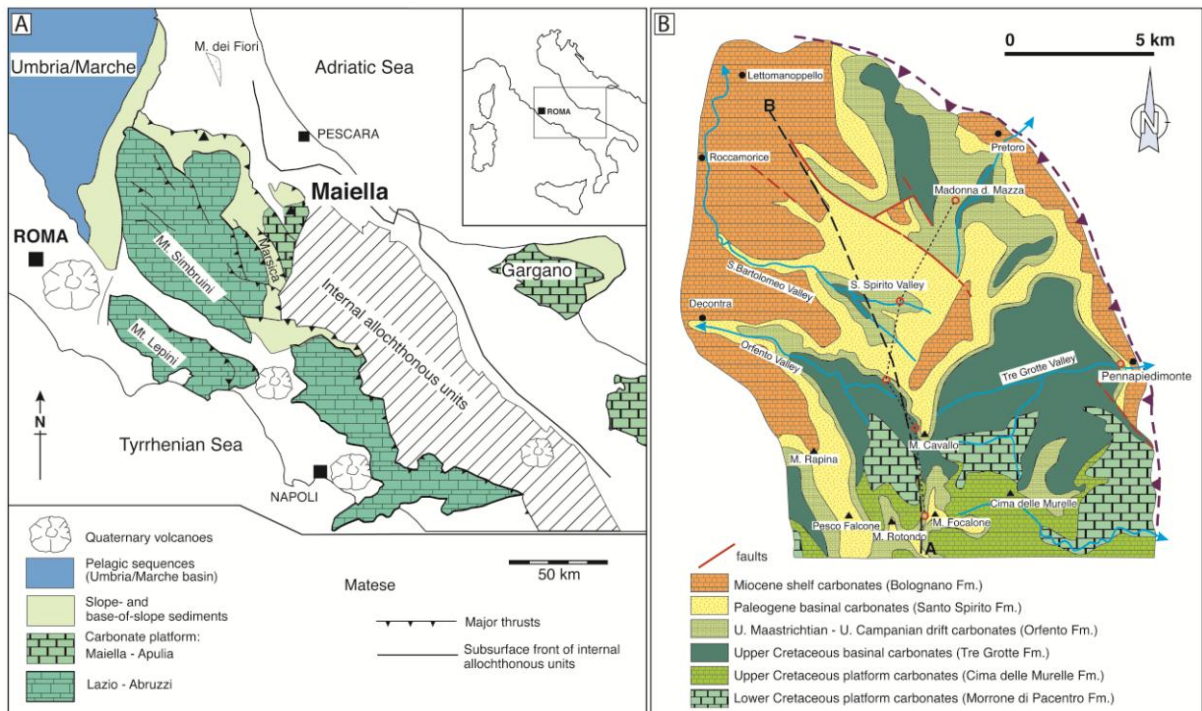
Fig. 25. Schematic display of the Maiella delta drift as plan view and dip and strike cross-section. Descriptions of the different elements are given in the text.

Table 1. Facies in the Orfento Formation

	<b>Facies</b>	<b>Bedding and sedimentary structures</b>	<b>Rock type and depositional texture</b>	<b>Grain type and composition</b>	<b>Wedge position and sedimentary processes</b>
Fa1	Mudstone to wackestone	Draping beds (1 to 2 cm), bioturbation, current ripples	Mudstone to wackestone	Micrite, silt-sized skeletal debris	Proximal to distal wedge. Low-energy drape from suspension, burrow fill, traction currents
Fa2	Fine-grained bioclastic grainstone	Parallel beds (10 to 20 cm), tangential downlaps, bioturbation	Grainstone to packstone	Silt to fine calcareous sand from rudist shells	Proximal to distal wedge. Sediment-laden currents
Fa3	Wavy-bedded bioclastic grainstone	Wavy and parallel beds (10 to 30 cm) typically in packages 5 to 10 m thick, foresets, ripples	Grainstone	Medium to coarse sand-sized skeletal fragments	Middle to distal wedge. Migrating sand waves and current reworking
Fa4	Massive bioclastic grainstone	Thin (5 to 10 cm), up to 5 m thick beds, bioturbated, mud drapes	Grainstone, with few packstones	Fragments of skeletal debris	Proximal to distal wedge. Various processes, bedload transport, (hyperpycnal) turbidity currents
Fa5	Bioclastic grainstone with cross-bedding and foresets	Parallel and even beds (up to 2 m), unidirectional foresets, hummocks, festoon-like	Coarse skeletal grainstone to packstone	Fine and coarse rudist fragments	Feeder channel, proximal to distal wedge. Sediment-laden currents, supercritical flows
Fa6	Graded bioclastic grainstone.	Parallel beds (20 to 50 cm), with erosive base, grading, ripples, water escape structures	Fine-grained bioclastic grainstone	Rudist fragments, minor intraclasts and large benthic foraminifera	Proximal to distal wedge. Turbidity currents (hyperpycnal)

Fa7	Massive grainstone with ripples and muddy top	Parallel beds (10 to 60 cm), massive to parallel laminations with ripple tops	Grainstone with mudstone cap	Medium to coarse sand-sized skeletal fragments (rudists)	Channel fill and proximal wedge. High-density turbidity current
Fa8	Grainstone with lithoclasts	0.5 to 1.0 m thick beds, crudely stratified with clasts	Grainstone, pebbles	Calcareous sand from rudist shells; rounded and angular grainstone and mud/wackestone clasts	Proximal to distal wedge. 'Cannibalization' of grainstone beds by currents; rip-up clasts, traction carpets
Fa9	Intraformational conglomerate and breccia.	Lenticular conglomerate beds amalgamated into 10 to 30 m thick channel fills with cut and fill geometry	Conglomerate with intraformational carbonate sand clasts. Matrix is grainstone	Clasts of bioclastic grainstone of rudist debris	Channel, proximal wedge. High-density turbidity current deposits; rip-up clasts, traction carpets.
Fa10	Breccia with convex upward relief	Lenticular with uneven top (2 to 4 m); unsorted platform clasts, angular to rounded	Platform clasts and deformed carbonate sand clasts of variable size (1 to 50 cm). Matrix: medium to coarse rudist grainstone	Matrix is rudist fragments. Clasts are intraclasts and loose bioclastic rudist debris, lithoclasts (from underlying formation)	Feeder channel and proximal wedge. High-density turbidity current deposits, reworking by currents





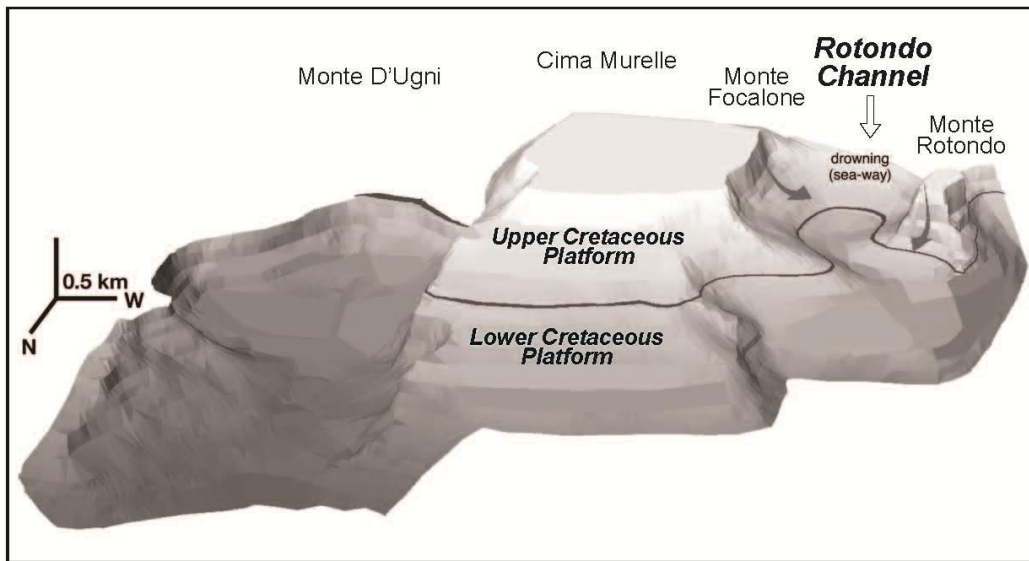
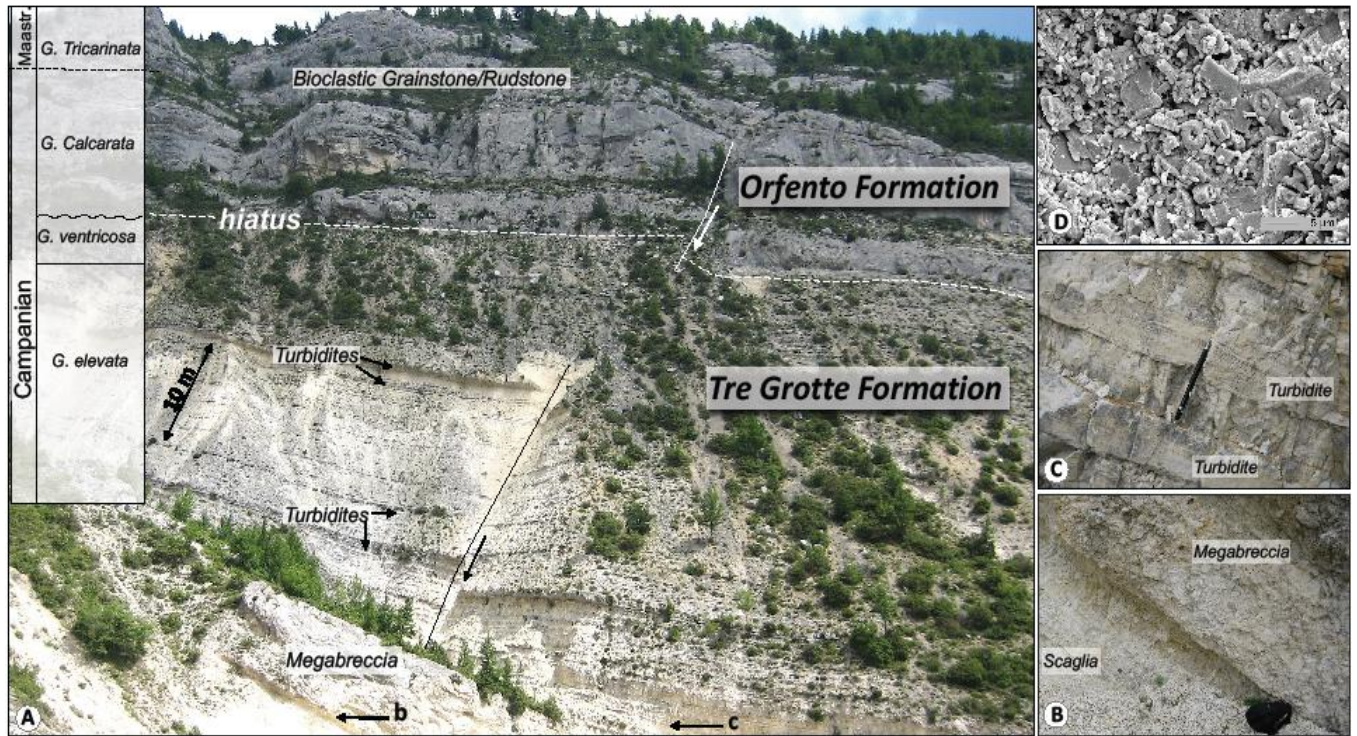
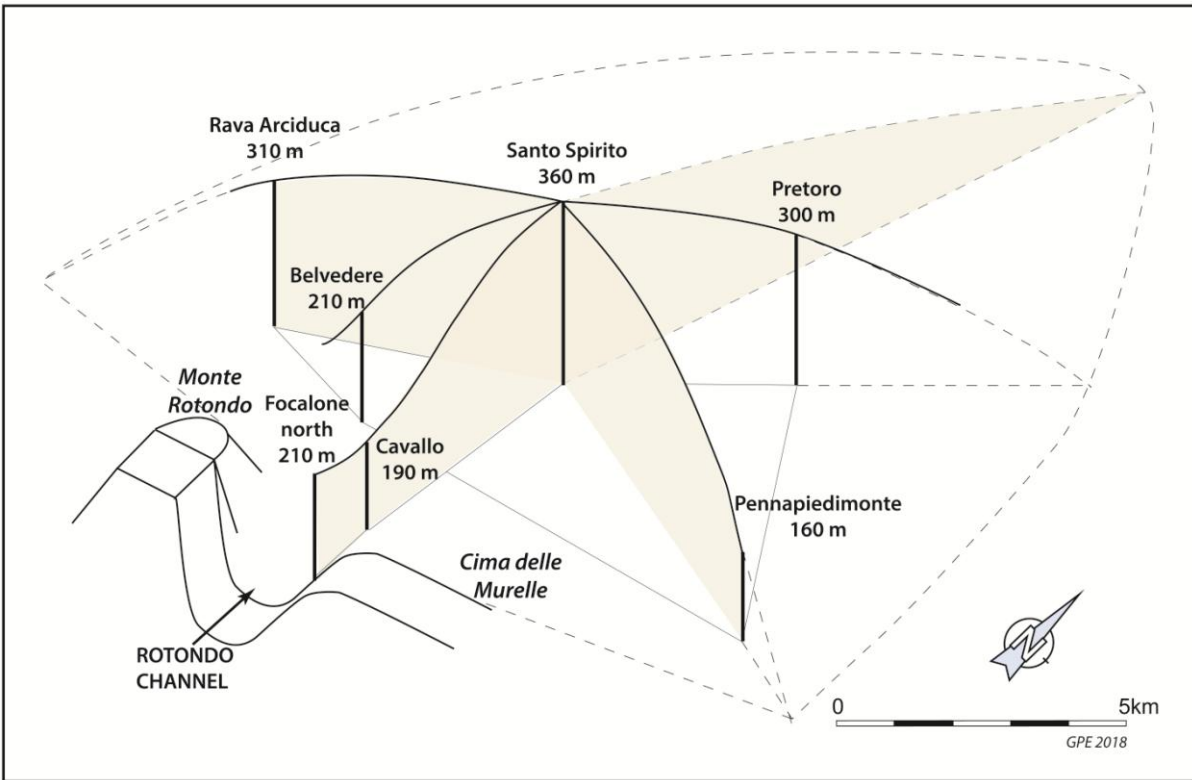
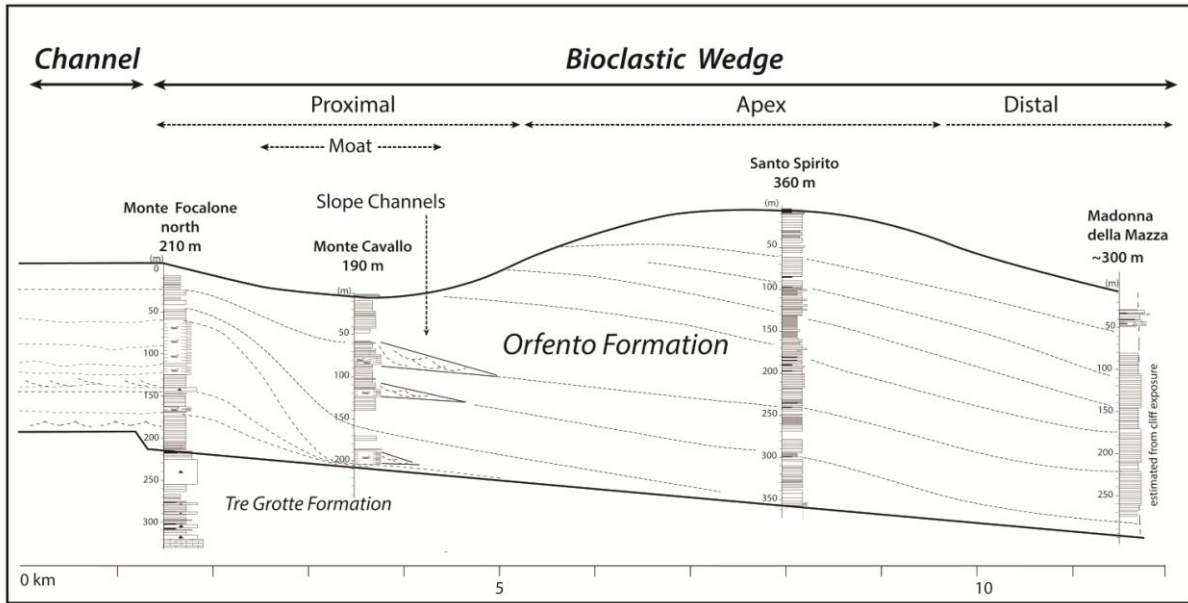


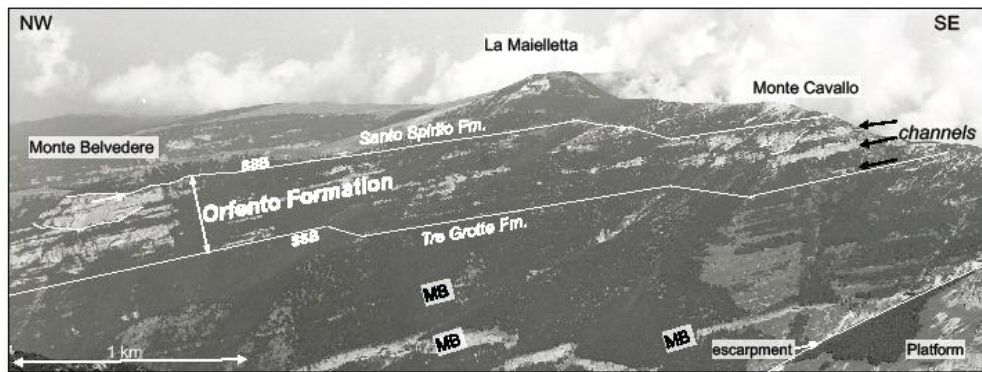
Figure 3: Eberli et al

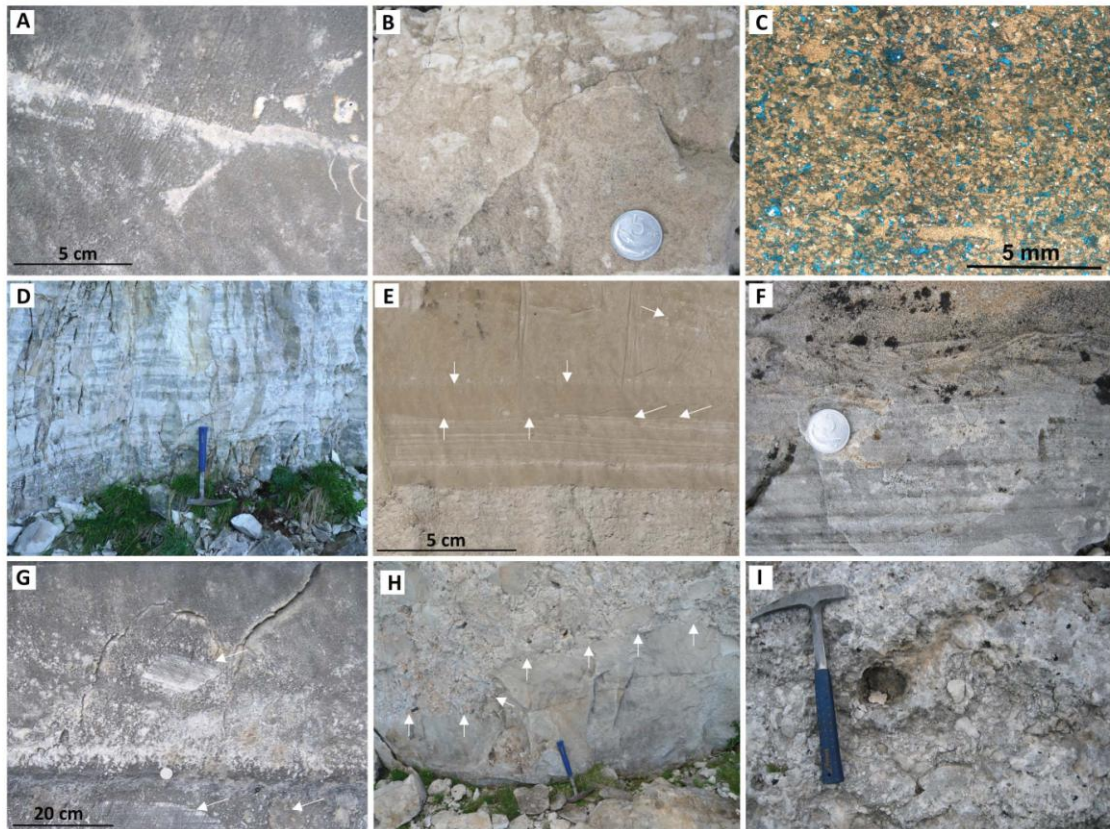


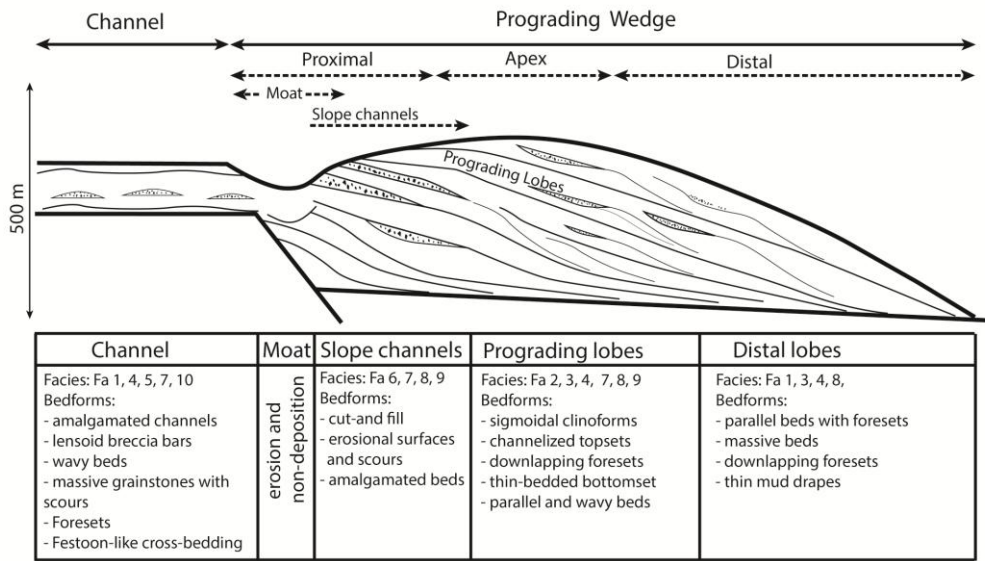


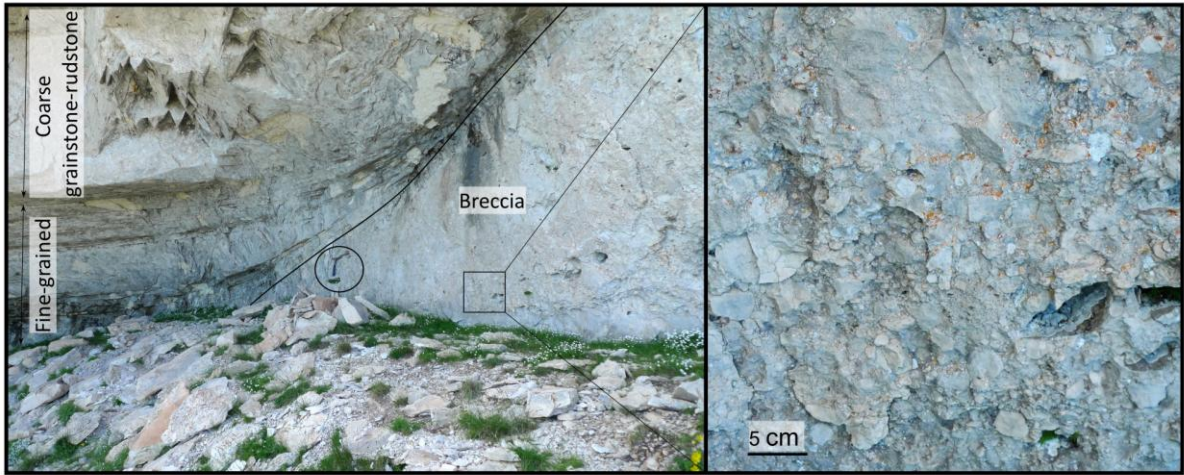


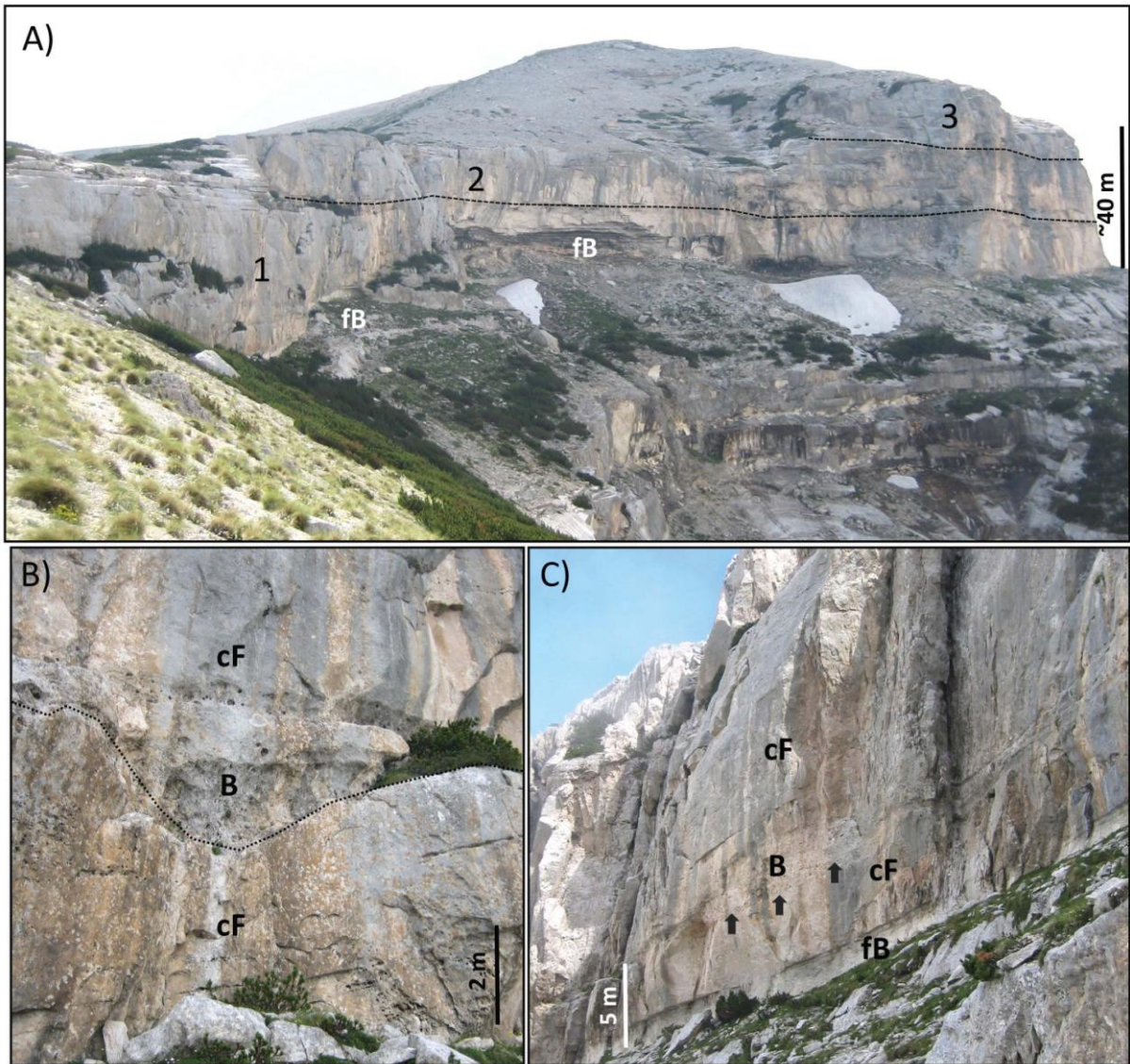


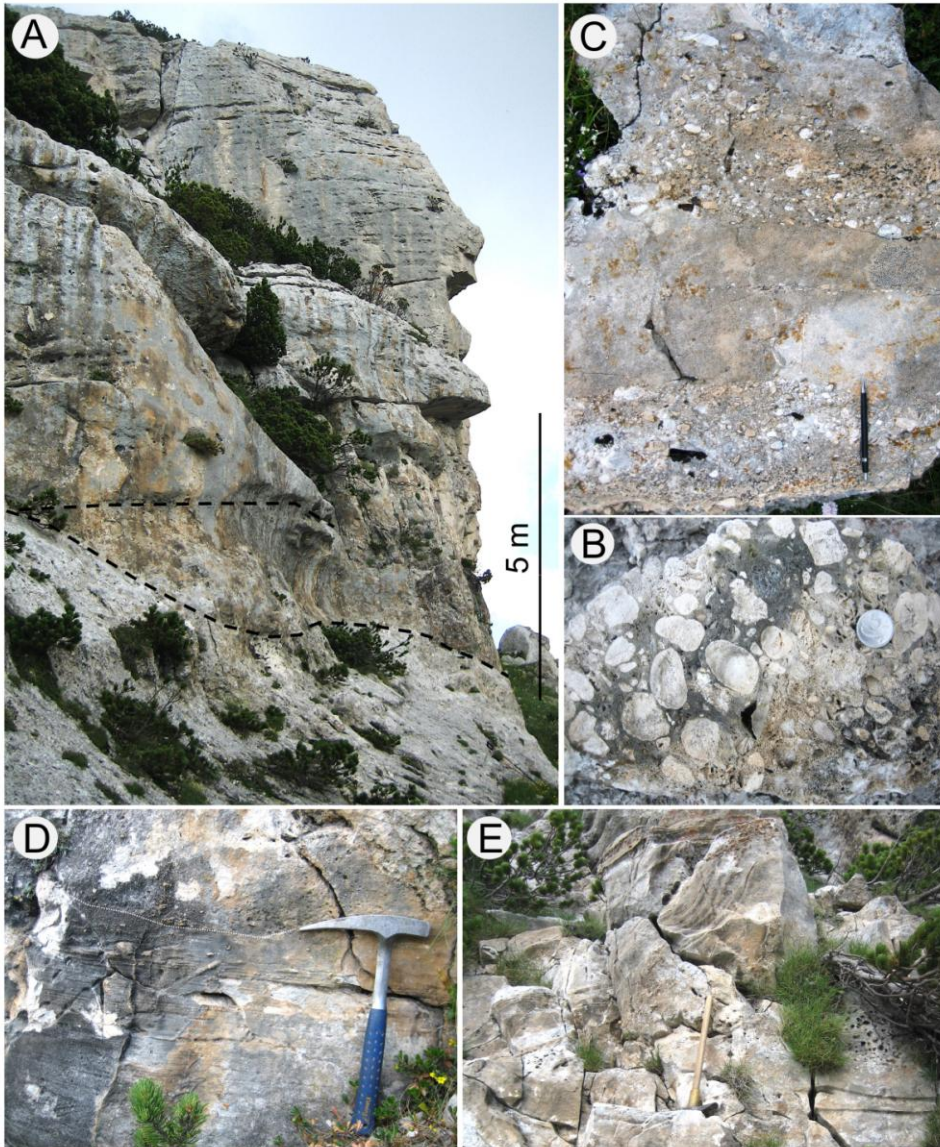












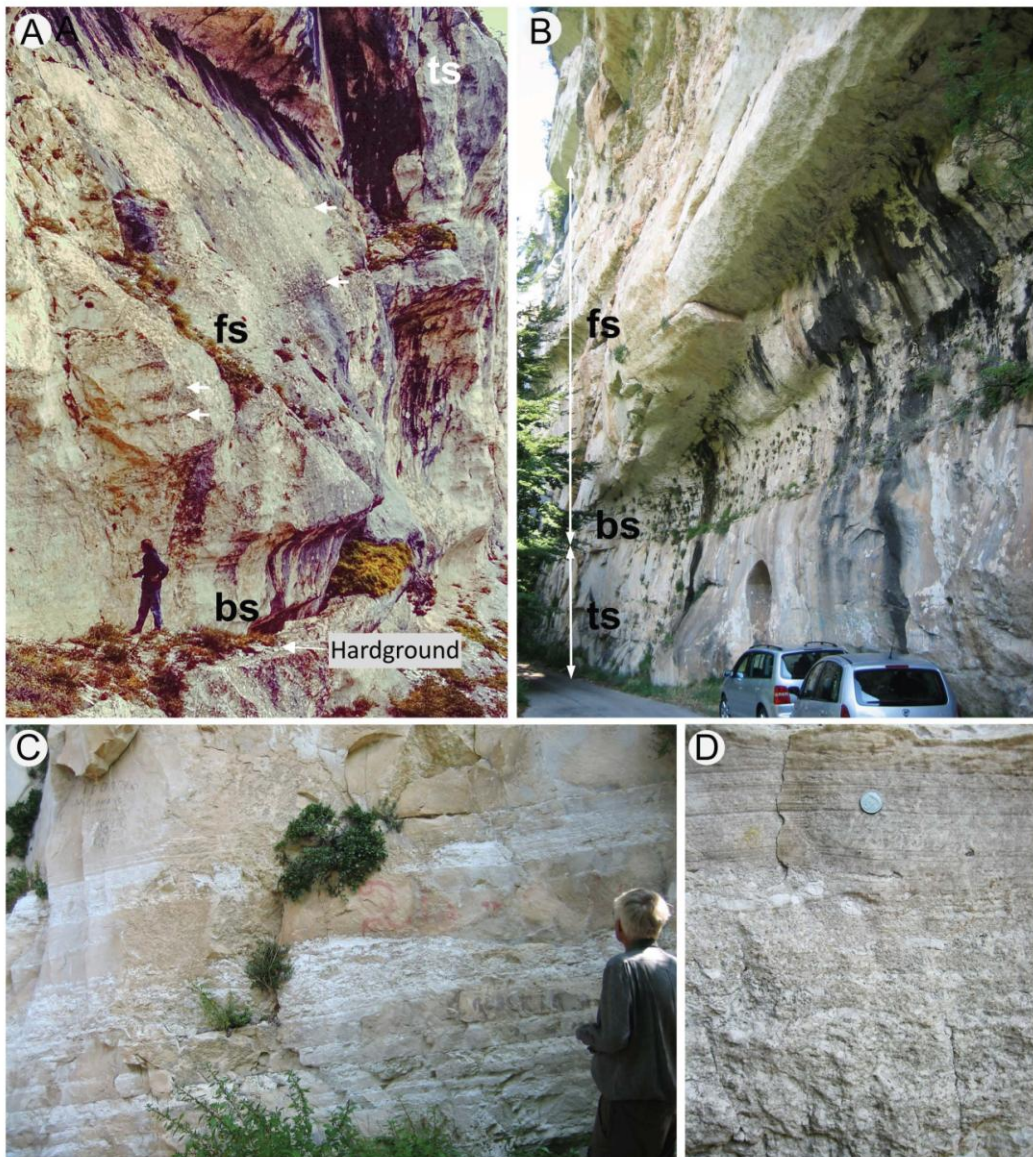


Figure 13: Eberli et al



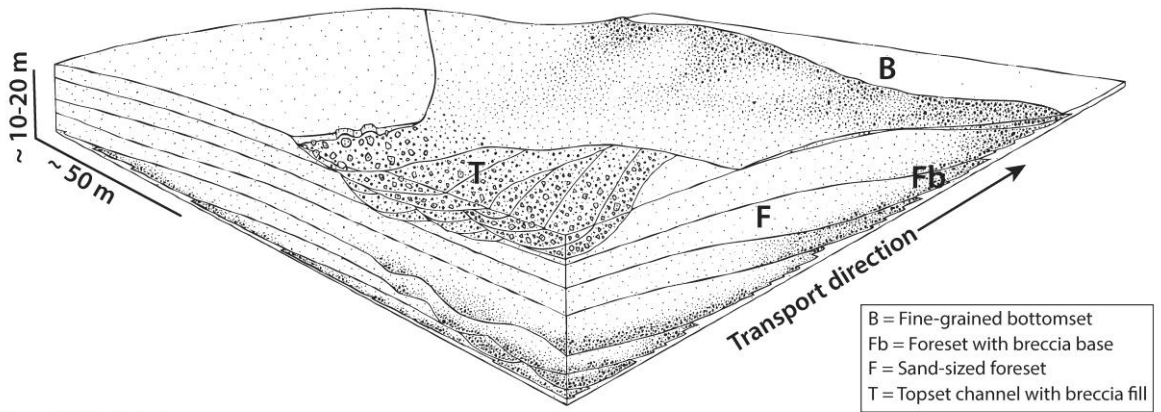
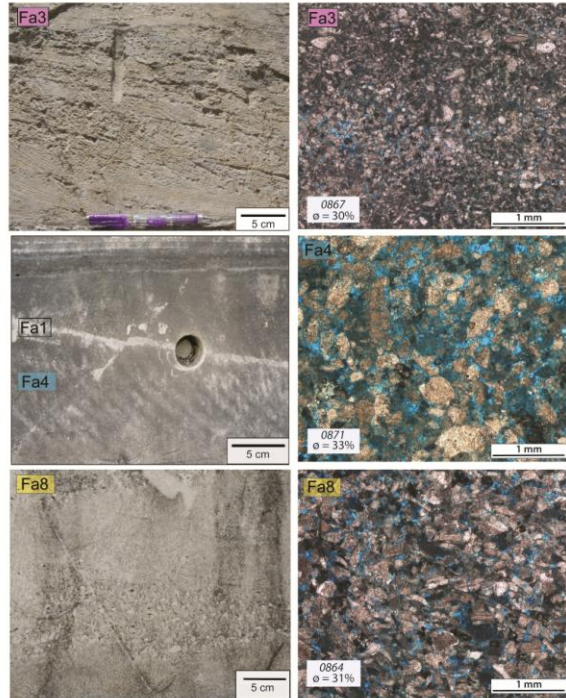
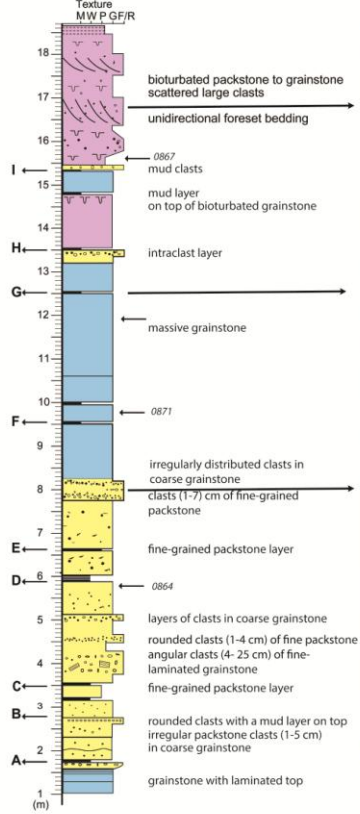


Figure 14: Eberli et al.

### Madonna della Mazza



Fa8 Grainstone with lithoclasts  
Fa1 Thin layer of wackestone  
Fa4 Massive grainstone  
Fa3 Bioturbated packstone/grainstone

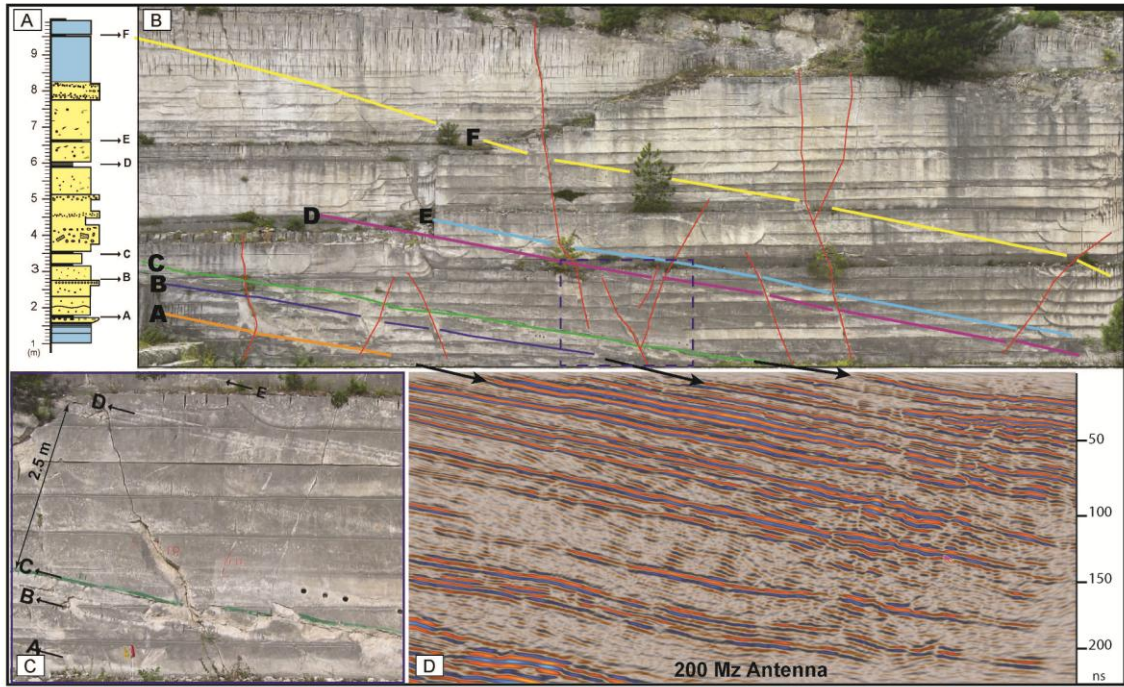
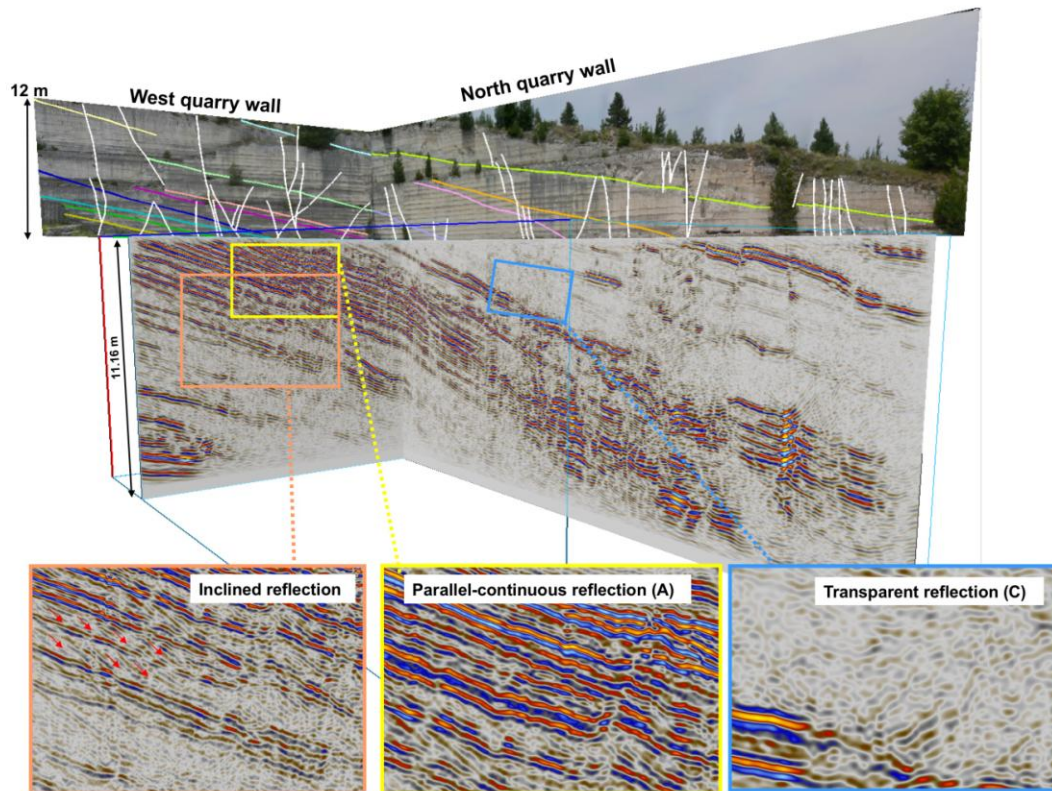


Figure 16: Eberli et al.



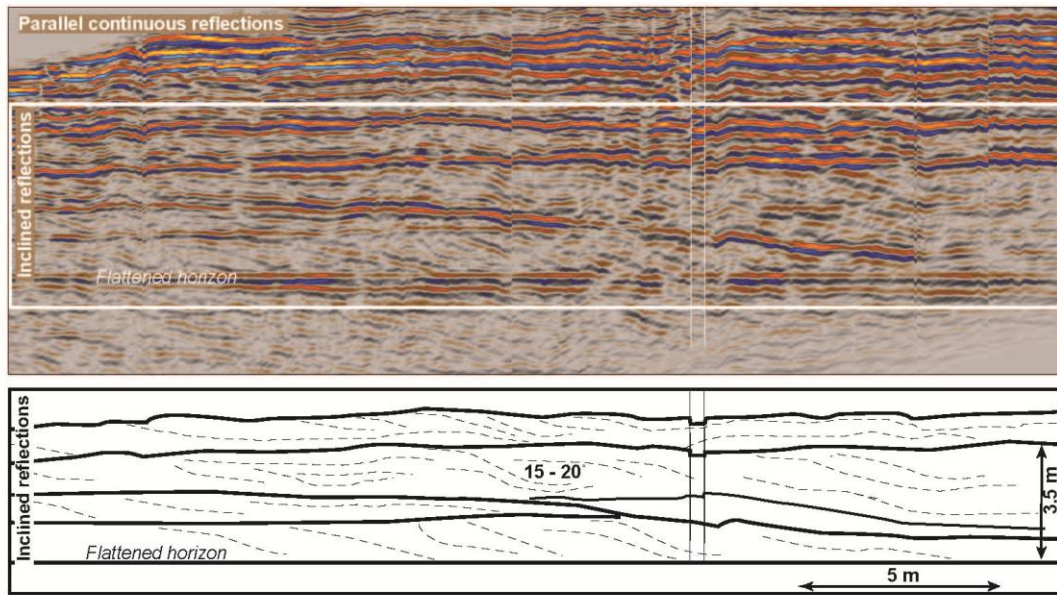
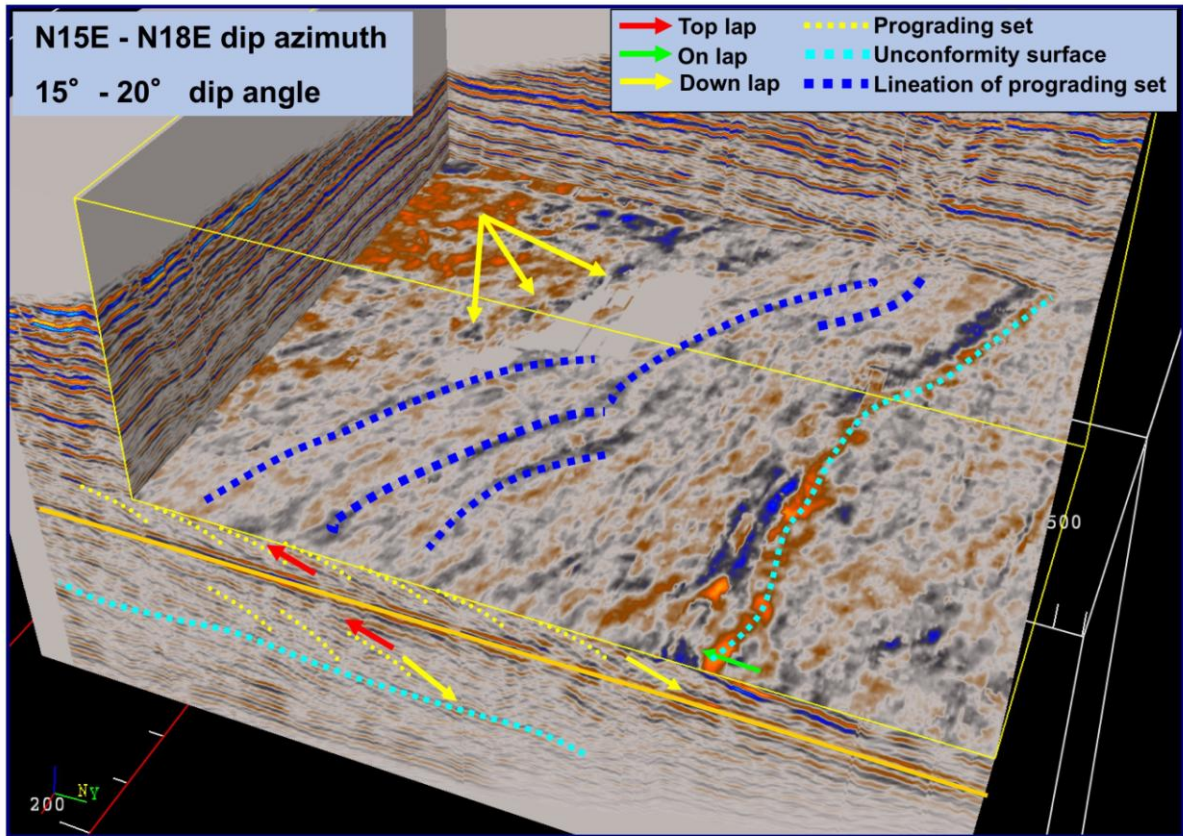
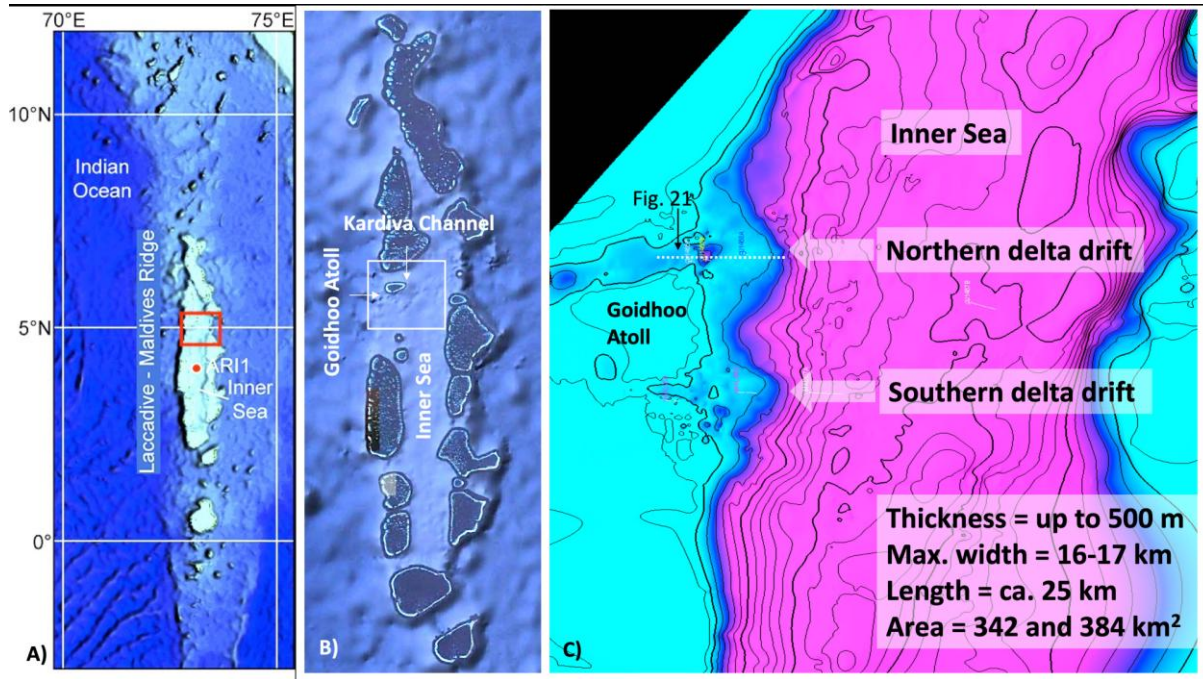


Figure 18: Eberli et al





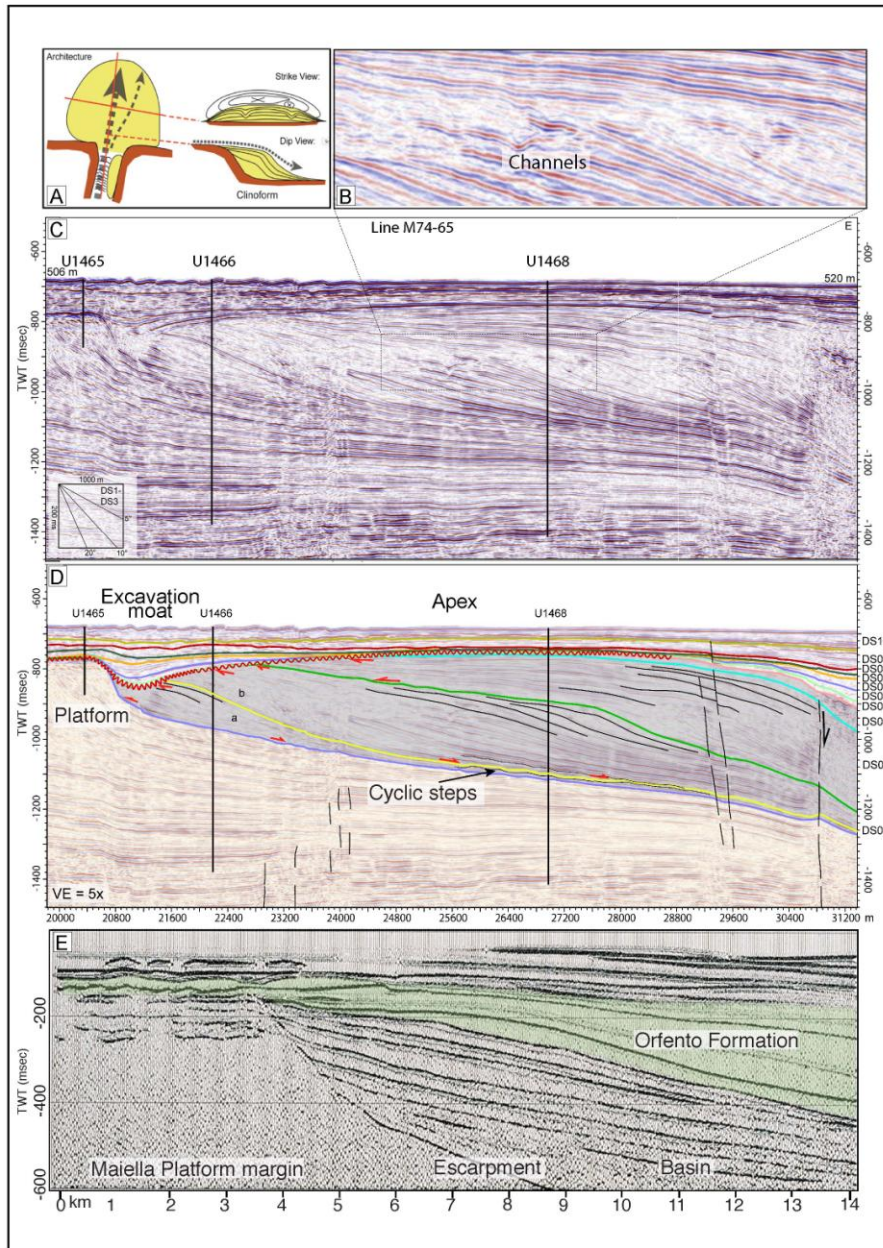
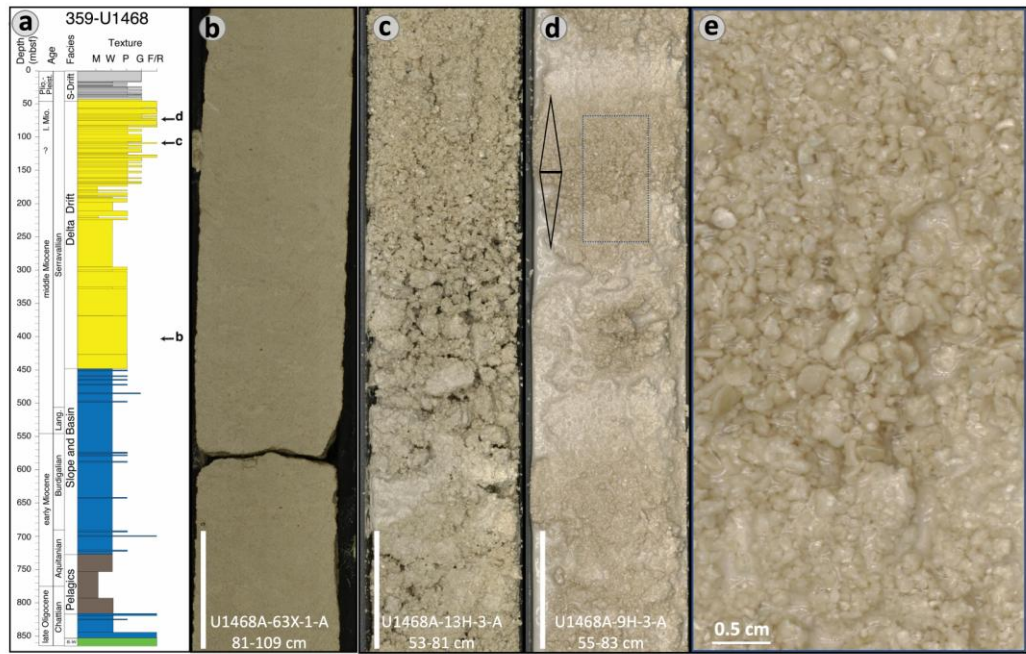
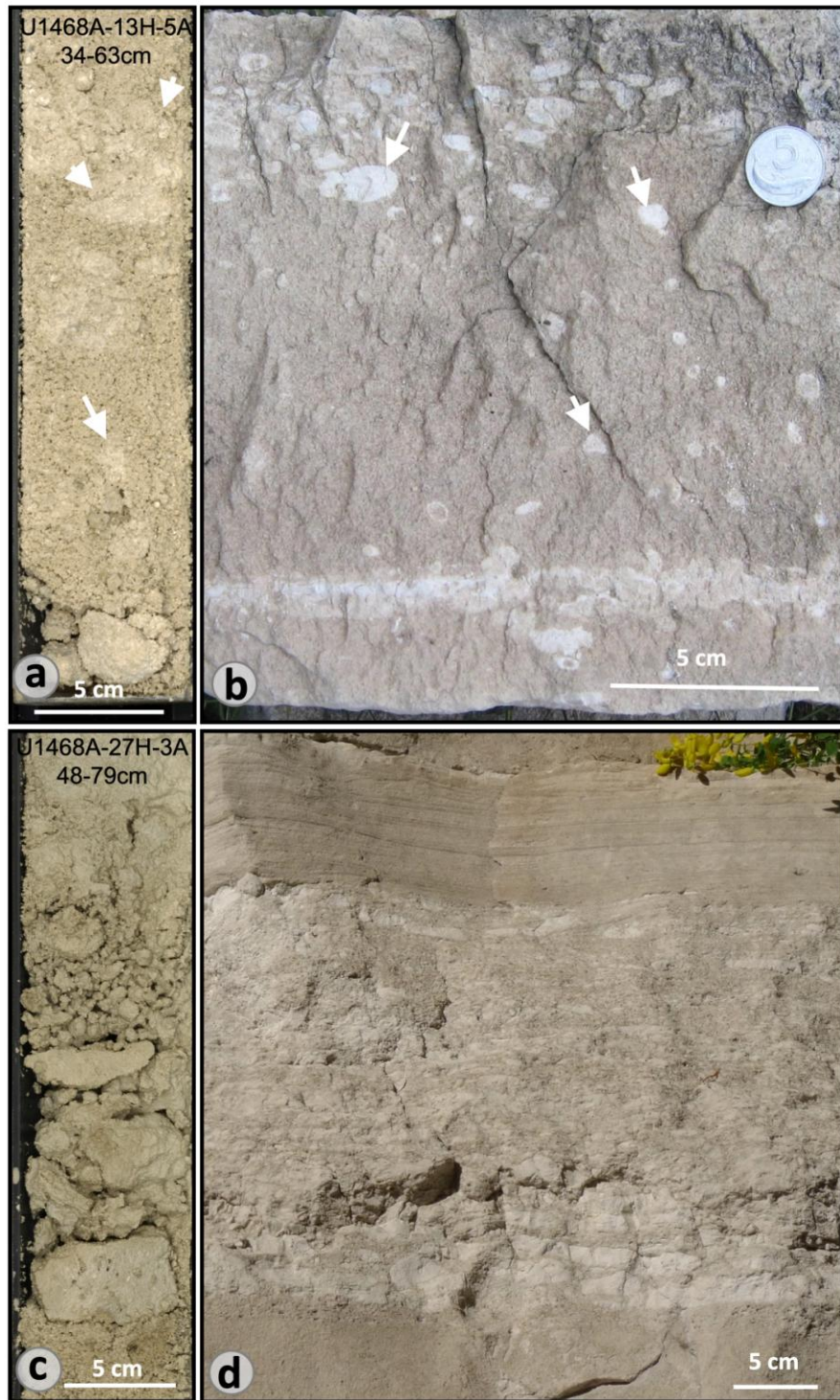


Figure 21; Eberli et al.







### Bioclastic Maiella Delta Drift

